Effects of Range of Motion on Skeletal Muscle Hypertrophy and Molecular Adaptations in Resistance-Trained Men

by

Daniel L. Plotkin

A dissertation submitted to the Graduate Faculty of
Auburn University
in partial fulfillment of the
requirements for the Degree of
Doctor of Philosophy in Kinesiology

Auburn, Alabama
August 8, 2026

Keywords: muscle hypertrophy, range of motion, molecular signaling

Approved by

Michael Roberts, PhD, Chair, Endowed Alumni Professor of Kinesiology, Auburn University
Andreas N. Kavazis, PhD, Professor of Kinesiology, Auburn University
Ryan Babl, PT, DPT PhD, Assistant Professor of Kinesiology, Auburn University
Christopher B. Mobley, Ph.D. Assistant Clinical Professor of Kinesiology, Auburn University
Darren T. Beck, PhD, Associate Dean for Biomedical Affairs and Research &
Discipline Chair and Associate Professor for Cell Biology and Physiology,
Edward Via College of Osteopathic Medicine

Abstract

This study examined how lengthened partial (LP) versus full range of motion (FULL) lower-body resistance training affects acute post-exercise signaling and chronic hypertrophy and cellular adaptations of the vastus lateralis (VL) muscle in resistance-trained men. Eight men (22±1 years old, 5.6±1.4 years training experience) completed a crossover study whereby VL biopsies were collected pre-exercise and 0, 3, and 24 hours following LP and FULL leg extension bouts for transcriptomic and anabolic signaling analyses (Experiment 1). Another 16 men (26±5 years old; 8.0 ± 4.9 years training experience) completed an 8-week, twice-weekly lower-body intervention using a within-subject contralateral limb design (Experiment 2). One leg was randomly assigned to FULL and the contralateral leg to LP training across three exercises (leg press, leg extension, and lying leg curl). Pre- and post-intervention outcomes included VL muscle cross-sectional area (mCSA) summed across five equidistant MRI-derived transverse and mid-thigh biopsy outcomes. Condition × Time interactions for all outcomes were assessed using linear mixed-effects models. In Experiment 1, both conditions produced similar time-dependent changes in the VL transcriptome and anabolic signaling, but minimal between-protocol interactions. In Experiment 2, VL summed mCSA significantly increased over time (mean change: 9.3 cm^2, 95% CI [6.8, 11.8], P<0.001), but there was no clear evidence of differential change between LP and FULL (LP − FULL change: −1.4 cm^2, 95% CI [−6.1, 3.4], P = 0.640). Additionally, no significant interactions existed for type I fiber CSA (P=0.476), type II fiber CSA (P=0.350), type I fiber myonuclei (P=0.813), type II fiber myonuclei (P=0.589), type I and II satellite cell number (P=0.102 and P=0.797, respectively), or total

RNA content (P=0.537). In conclusion, these data suggest that LP and FULL resistance training when executed within a typical lower body program broadly elicit similar acute and chronic VL responses in previously trained men.

Artificial Intelligence (AI) Use Disclosure Statement

In the preparation of this thesis/dissertation, the following Artificial Intelligence (AI) tools were used: Claude by Anthropic. These tools were used primarily to inform language and grammar. The author acknowledges full responsibility for the intellectual content of this work and has ensured that all AI-assisted sections have been reviewed and revised for accuracy and appropriate academic style. All AI-generated content was reviewed and validated for relevance, appropriateness, and accuracy before incorporation into the final document to maintain the scholarly integrity of this research.

Digital Accessibility Use Disclosure Statement

In the preparation of this thesis / dissertation, the following digital accessibility tools were used to ensure this document complies with federal requirements: accessibility tool in Adobe. The author acknowledges full responsibility for the intellectual content of this work and has made a good faith effort to comply with digital accessibility requirements in publishing, wherein the nature of the content does not significantly change in order to do so. Furthermore, all content has been reviewed and revised to meet these requirements prior to final publication.

Acknowledgements

I would like to express my deepest gratitude to the people who made this work possible and made the journey worthwhile.

To Merlina, you make my life better in every way. Your unwavering support throughout this process has meant more than I can put into words.

To my advisor, Dr. Michael Roberts, you are quite possibly the kindest person I know, and I am incredibly fortunate to have had you in my corner both in and out of the lab. Thank you for your mentorship, your generosity, and for always making time.

To my committee, thank you for your patience, your guidance, and your willingness to be there whenever I needed to pilot something, talk through my future, or simply have a conversation. Your support extended well beyond the academic, and I am grateful for it.

To my lab mates, thank you for striking the balance between being there when it mattered and knowing when it was time to goof off. Our dry lab conversations and wet lab shenanigans will not be forgotten. A special thank you to Dakota Teide, whose enthusiasm for training and hypertrophy science made this work more enjoyable and whose contributions were integral to seeing it through. Few people I know personally care as much about this weird thing we call muscle hypertrophy as he does, and that's saying something.

Table of Contents

List of Figures

List of Abbreviations

LP, Lengthened partial

FULL, Full range of motion

VL, Vastus lateralis

MRI, Magnetic resonance imaging

mCSA, Muscle cross-sectional area

fCSA, Fiber cross-sectional area

SC, Satellite cell

mTORC1, Mammalian target of rapamycin complex 1

ROM, Range of motion

PRE, Pre-intervention / pre-exercise

POST, Post-intervention / post-exercise

0h POST, Immediately post-exercise

3h POST, 3 hours post-exercise

24h POST, 24 hours post-exercise

RF, Rectus femoris

FAK, Focal adhesion kinase

S6K1, Ribosomal protein S6 kinase beta-1

4E-BP1, Eukaryotic translation initiation factor 4E-binding protein 1

rDNA, Ribosomal DNA

RNA, Ribonucleic acid

mRNA, Messenger RNA

LMM, Linear mixed-effects model

CI, Confidence interval

IRB, Institutional Review Board

DXA, Dual-energy x-ray absorptiometry

10RM, 10-repetition maximum

BIA, Bioelectrical impedance analysis

IHC, Immunohistochemistry

OCT, Optimal cutting temperature compound

PVDF, Polyvinylidene fluoride

TBST, Tris-buffered saline with Tween-20

HRP, Horseradish peroxidase

BCA, Bicinchoninic acid

BSA, Bovine serum albumin

DAPI, 4',6-diamidino-2-phenylindole

PBS, Phosphate-buffered saline

DEPC, Diethyl pyrocarbonate

TAC, Transcriptome Analysis Console

PANTHER, Protein ANalysis THrough Evolutionary Relationships

ANOVA, Analysis of variance

FIM-ID, Fluorescence imaging of myofibrils with image deconvolution

Chapter 1: Introduction

Skeletal muscle hypertrophy in response to resistance training is primarily driven by mechanical overload [1]. However, hypertrophic adaptations may depend on characteristics of the mechanical stimulus, including tension magnitude, the muscle length at which tension is applied, and the spatial distribution of strain within the muscle. A growing body of evidence suggests that training at longer muscle lengths may produce greater hypertrophy than training at shorter lengths. Studies comparing biarticular muscles trained at different static joint positions show a relatively consistent pattern. For the hamstrings, which span the hip and knee, training with greater hip flexion (seated hamstring curls) produces greater hypertrophy than training with less hip flexion (lying curls) after 12 weeks in both trained and untrained individuals [2]. Similarly, the rectus femoris (RF) exhibits greater growth when trained in conditions that lengthen the muscle at the hip, such as greater hip extension or a reclined position during leg extensions [3]. For the gastrocnemius, training with the knee extended produces greater hypertrophy than training with the knee flexed, consistent with knee extension increasing gastrocnemius length [4]. Collectively, these findings suggest that biarticular muscles may respond favorably when trained in a more lengthened position.

Beyond static positions, several studies have compared partial range of motion (ROM) training that emphasizes the lengthened versus shortened portion of the movement. In the calf musculature, lengthened partials (LP) produce greater hypertrophy than shortened partials and, in some cases, greater hypertrophy than full range of motion (FULL) training [5]. For the quadriceps, evidence also generally favors longer muscle

lengths, though findings are more mixed. Deeper squat training produces greater vastus lateralis (VL) hypertrophy than shallower squats [6] and partials in a more lengthened position produce larger increases in quadriceps size than partials in a shortened position [7]. In contrast, some studies have reported similar hypertrophy between interventions that emphasize different ranges of motion, which may reflect sampling variability, differences in population, exercise execution, differences in response for a particular muscle, loading strategy, proximity to failure, or reaching a requisite muscle length beyond which differences are small or non-existent [8-11]. Importantly, the hypertrophic impact of emphasizing longer muscle lengths may not be uniform across muscles or exercises. In many resistance exercises, sets performed through a full range of motion tend to reach failure near the shortened position. As a result, a substantial portion of fatigue may accumulate when the muscle is relatively shortened, while the lengthened region may be comparatively underloaded.

Lengthened partial range of motion training alters this distribution by maintaining high tension specifically when the muscle is longer and may therefore be particularly relevant in exercises where the primary resistance challenge occurs at shorter muscle lengths. Despite accumulating evidence favoring lengthened-position training, several critical gaps remain. First, most studies have been conducted in untrained individuals, with relatively few controlled trials in resistance-trained populations. Second, many studies rely on ultrasound muscle thickness measured at one or two sites, whereas magnetic resonance imaging (MRI)-based cross-sectional area and volume assessments across the length of the muscle are rarely employed in range of motion research. Third,

limited work has examined altering range of motion in the context of exercises with differing resistance curves, which may influence where within the range of motion peak mechanical demands and fatigue occur. Fourth, fiber type-specific myofiber cross-sectional area (fCSA) as well as satellite cell content and ribosome content, both of which are critical mechanisms for skeletal muscle hypertrophy [12], have not been evaluated when comparing range of motion conditions in humans. Fifth, acute transcriptional responses nor anabolic signaling in response to lengthened-biased versus full range of motion resistance exercise have not been characterized, limiting identification of candidate genes and pathways. Finally, specific muscle groups remain understudied, including the absence of controlled studies isolating hamstring partial range of motion training at long muscle lengths.

Therefore, the purpose of this dissertation is to perform an acute and chronic intervention in resistance-trained men using unilateral within-subject designs to address these gaps. In Experiment 1 (acute bout), participants will perform leg extensor resistance training for one bout whereby one leg is assigned full range of motion training (FULL), and the contralateral leg is assigned lengthened partial training (LP) with 4 sets of leg extensions. VL biopsies will be collected prior to (PRE) as well as immediately following (0h POST), 3 hours following (3h POST), and 24 hours following each bout (24h POST). Outcomes will include global mRNA assessments (i.e., the protein-coding transcriptome) as well as phosphorylated mammalian target of rapamycin complex 1 (mTORC1) and Hippo signaling protein targets. This study will be the first human investigation to examine range of motion resistance training effects on molecular outcomes in trained individuals.

Experiment 2 will involve an independent cohort of participants who will perform 8 weeks (2 days per week) of unilateral leg resistance training whereby one leg is assigned to FULL and the contralateral leg to LP across three exercises including leg press, leg extension, and lying leg curl. This study will also be the first human investigation to examine range of motion resistance training effects using MRI-derived muscle cross-sectional area (mCSA) or VL biopsies to assess fCSA, satellite cell number, and total RNA content (a valid surrogate of ribosome content per wet tissue weight) in trained individuals.

Specific Aims

Experiment 1, Aim 1: Determine if VL molecular signature differences exist following one bout of full range of motion versus lengthened partial range of motion resistance training.

Experiment 2, Aim 1: Examine regional VL hypertrophy patterns between training paradigms via MRI-derived image analysis to determine whether lengthened partials produce differential regional growth compared to full range of motion resistance training.

Experiment 2, Aim 2: Assess fiber type-specific fCSA, satellite cell number, and total RNA content from VL biopsies to evaluate chronic cellular-level adaptations.

Experiment 2, Aim 3 (exploratory): Compare changes in whole-muscle size between full range of motion and lengthened partial range of motion training in the quadriceps, hamstrings, and gluteal muscles via MRI-derived image analysis.

Hypotheses

Experiment 1, Aim 1: Given the lack of molecular data in this area, I adopt the null hypothesis and assume that an acute bout of both training paradigms will elicit similar post-exercise transcriptomic and anabolic signaling alterations.

Experiment 2, Aims 1–3: I hypothesize that VL myofiber cross-sectional area, satellite cell number, and total RNA content will increase similarly between conditions. Furthermore, I hypothesize that whole muscle vasti, adductors, and gluteus maximus hypertrophy will be similar between conditions, whereas hamstrings and rectus femoris hypertrophy will be greater in the lengthened partial condition. This prediction is based on the premise that lengthened partials may confer a greater benefit for muscles that are underloaded at long muscle lengths during the intervention.

Significance

This project will generate evidence on how manipulating range of motion can optimize hypertrophy, while also deepening mechanistic insight into how muscle length during loading regulates fiber-level adaptations. The results will inform more efficient and effective resistance training prescriptions, provide practical options for individuals limited to specific movement ranges, and refine theoretical models of length-dependent muscle growth.

Chapter 2: Literature Review

Adaptation to Resistance Training and Skeletal Muscle Microstructure

Resistance training is an intervention with exceptionally high utility for improving the function of multiple organ systems and enhancing health across a wide range of contexts. It exerts positive effects throughout the body, with evidence showing improvements in cognitive function, insulin sensitivity, bone mineral density, mobility, and flexibility [13-17]. Resistance training also reduces the risk of cardiovascular disease, cancer, and all-cause mortality, even when performed alongside aerobic exercise [18].

Many of the adaptations that occur due to resistance training are in skeletal muscle. Skeletal muscle is an integrally important organ in the human body. Its principal role is to act as an actuator for bone, converting neural signals into mechanical force for movement, but its importance goes well beyond locomotion. Muscle plays central roles in glucose disposal, lipid metabolism, thermoregulation, and systemic homeostasis. Because of these functions, gaining and maintaining skeletal muscle mass is closely linked to improved metabolic health, reduced risk of chronic disease, and sustained physical independence across the lifespan [19, 20].

Because many of the health-promoting effects of resistance training originate in skeletal muscle, understanding these adaptations requires consideration of muscle's structural organization. While resistance training is a highly effective method for increasing skeletal muscle mass and function [1], where and how this mass is added is important to understanding function and implementing targeted and efficient interventions.

Sarcomere Structure and Organization. Skeletal muscle force production is rooted in the highly ordered structure of the sarcomere, the fundamental contractile unit of the myofibril. Sarcomeres are arranged end to end along the length of myofibrils, which themselves are aligned in parallel within the muscle fiber, forming a hierarchical organization that enables coordinated force generation across large cellular dimensions. A sarcomere is composed primarily of thick filaments, containing myosin, and thin filaments, composed of actin along with regulatory proteins such as troponin and tropomyosin.

This precise organization not only supports efficient contractile function but also establishes the structural framework through which mechanical forces are distributed within the muscle fiber. The continuity between sarcomeres, myofibrils, cytoskeletal networks, and extracellular structures ensures that mechanical loading at the whole-muscle level is experienced at the level of individual sarcomeres. Force generation occurs through cyclic interactions between myosin heads and actin binding sites, a process known as the sliding filament theory [21]. Importantly, the spatial arrangement of the filaments determines the degree of actin–myosin overlap and, consequently, the potential for active force production [22]. Understanding this organization is therefore essential for interpreting how variations in mechanical loading conditions, including differences in muscle length during contraction, may influence the internal mechanical environment that drives adaptation.

Thin and Thick Filament Length. Ultrastructural studies consistently report thick filament lengths of approximately 1.6 μm, with minimal variation across species, muscles,

or fiber types [23, 24]. To date, no evidence suggests meaningful differences in thick filament length attributable to functional specialization or mechanical loading history. In contrast, thin filament length is not conserved in such a manner. Comparative work has demonstrated systematic differences in thin filament length across species, with humans exhibiting longer thin filaments than commonly studied amphibian and rodent models [25]. More recently, direct evidence has shown that thin filament length varies within human skeletal muscle. Gokhin and colleagues demonstrated that thin filament length differs across fiber types in humans, with slow-twitch fibers exhibiting longer thin filaments than fast-twitch fibers [26]. Reported values in human muscle span approximately 1.19 to 1.37 μm, indicating substantial variability relative to thick filament length. These findings establish that thin filament length is a regulated structural feature that differs across fiber types and potentially across muscles with differing functional demands. Despite this variability, there is currently no evidence that thin filament length adapts in response to resistance training or altered mechanical loading. No longitudinal human studies have examined whether chronic loading modifies thin filament length, nor has training-induced remodeling of thin filaments been clearly demonstrated in animal models. It may be that thin filament length is a muscle- and fiber-type–specific structural parameter that defines baseline sarcomere operating characteristics rather than an established target of adaptation. However, evidence is unavailable to draw this conclusion with certainty.

Together, these findings indicate that thick filament length is largely conserved, whereas thin filament length varies across human muscle fibers in a manner consistent with functional specialization. This structural heterogeneity implies that this is one reason

that muscles and fiber types operate on distinct regions of the force–length curve. The absence of direct evidence regarding thin filament length plasticity represents an important unresolved question in skeletal muscle biology.

Adaptations to Sarcomere Number and Length. Early increases in fascicle length do not necessarily reflect immediate sarcomerogenesis. In both animal and human models, short-term exposure to high forces at long muscle lengths or eccentric contractions may initially increase resting sarcomere length without a substantial rise in serial sarcomere number. Human microendoscopy studies using Nordic hamstring training illustrate this pattern. After 3 weeks, fascicle length increased largely via elongation of existing sarcomeres, whereas longer interventions showed clearer increases in serial sarcomere number [27, 28].

Although serial sarcomere addition in humans is becoming increasingly supported, uncertainty remains regarding the specific conditions under which this adaptation occurs [29, 30]. Rodent models indicate that contractions performed at longer muscle lengths provide a strong stimulus for increasing sarcomere number in series; however, current human data are insufficient to draw definitive conclusions on the contribution of eccentric contractions [30]. Several resistance training studies have reported changes in fascicle length from resistance training at longer lengths [29], but findings are inconsistent and protocols and muscles measured are heterogeneous. Moreover, in the absence of direct sarcomere length measurements, it is not possible to determine whether observed changes in fascicle length reflect increases in sarcomere length, increases in sarcomere number, or a combination of both.

Myofibril Adaptations to Loading. Skeletal muscle hypertrophy ultimately reflects structural remodeling of the contractile apparatus. While increases in whole-muscle size are commonly described at the macroscopic level, these changes arise from adaptations at the microscopic and ultrastructural levels within individual muscle fibers. A key question in muscle biology is how the contractile machinery itself expands in response to mechanical overload. Current evidence indicates that growth is mediated primarily through increases in myofiber cross-sectional area, but the specific ultrastructural processes underlying this enlargement remain incompletely defined.

At the ultrastructural level, the majority of the myofiber volume is occupied by myofibrils, which are composed of sarcomeres arranged in series and aligned in parallel across the fiber. Thus, an increase in myofiber cross-sectional area must involve expansion of this myofibrillar lattice. Two non-mutually exclusive mechanisms have been proposed: enlargement of pre-existing myofibrils and the addition of new myofibrils. Until recently direct in vivo evidence distinguishing between them did not exist. Recent work employing Fluorescence imaging of myofibrils with image deconvolution (FIM-ID) has provided the first direct structural evidence addressing this question [31]. Using this approach, investigators quantified myofibril number, size, and spatial organization within single muscle fibers following mechanical overload. The results demonstrated that increases in myofiber cross-sectional area were driven predominantly by an increase in the number of myofibrils arranged in parallel, with minimal change in the cross-sectional area of individual myofibrils. Importantly, myofibrillar packing density and lattice organization

were largely preserved despite substantial fiber hypertrophy, indicating that growth occurs through coordinated addition of contractile units rather than indiscriminate expansion of existing structures. These findings provide support for myofibrillogenesis as a primary mechanism underlying resistance training–induced hypertrophy. Rather than thickening existing myofibrils, mechanically loaded muscle fibers appear to expand their contractile capacity by assembling new myofibrils alongside pre-existing ones, thereby increasing force-generating potential while maintaining structural integrity. This finding suggests that sarcoplasmic expansion is likely in conjunction and in support of myofibrillar expansion.

Sarcoplasmic and Myofibrillar Components of Muscle Fiber Hypertrophy. Some experimental work has raised the possibility that resistance training may bias expansion toward specific intracellular compartments [32]. Limited evidence involving very high training volumes indicates that disproportionate increases in sarcoplasmic protein content, intracellular fluid, or other non-contractile components relative to myofibrillar protein can occur [33]. These observations have led to the suggestion that resistance exercise can, under certain conditions, produce a transient dissociation between increases in fiber size and expansion of the contractile apparatus. However, when considered alongside the totality of current evidence, compartmental biases, if present, are likely temporary under normal resistance training conditions and in the long term [34]. Recent human work using phalloidin staining of VL biopsies has even reported that blood flow restriction with resistance training does not alter the ratio of sarcoplasmic to myofibrillar fractions [35]. And as mentioned prior, FIM-ID has confirmed the persistence of a maintained ratio after normal resistance training conditions [31]. Consistent with this

interpretation, measures of specific tension are generally preserved following hypertrophy once swelling is accounted for, indicating that force production scales appropriately with fiber size rather than being diluted by non-contractile expansion [36]. Together, these findings counter the existence of a stable or functionally meaningful separation between muscle size and myofibrillar accretion in resistance-trained muscle.

Importantly, expansion of the sarcoplasmic compartment should not be interpreted as non-functional or antagonistic to contractile growth. The sarcoplasm contains the enzymatic, ribosomal, and organelle systems required to sustain repeated cycles of protein synthesis and remodeling. Increases in total RNA content, ribosome biogenesis, and translational capacity observed with mechanical overload reflect necessary adaptations that support continued myofibrillar protein accretion rather than replacing it. From this perspective, hypertrophy is best conceptualized as coordinated remodeling across contractile, structural, and metabolic compartments, with potential transient mismatches in relative expansion likely resolving as training progresses.

Conclusion. Overall, the current evidence indicates that resistance training–induced hypertrophy reflects coordinated and proportional growth of both myofibrillar and sarcoplasmic compartments rather than a lasting divergence between fiber size and contractile content. Concurrent expansion of sarcoplasmic and organelle components supports metabolic, translational, and calcium-handling machinery. Thus, muscle hypertrophy is best viewed as integrated remodeling across structural and metabolic domains, with contractile growth and supportive cellular adaptations progressing in parallel.

Muscle Macrostructure and Architectural Adaptations

While hypertrophy is rooted in remodeling of sarcomeres and myofibrils, these microscopic adaptations scale upward to alter the macroscopic architecture of the muscle. Whole-muscle morphology is defined not only by muscle volume or mCSA, but also by architectural features such as fascicle length and pennation angle. These properties determine how contractile material is arranged in space and strongly influence both force production and how growth manifests at the tissue level [34, 37].

Muscle fascicles are bundles of myofibers arranged at an angle relative to the line of pull of the tendon. Fascicle length reflects, in part, the number of sarcomeres arranged in series, whereas physiological cross-sectional area is determined primarily by the number of sarcomeres arranged in parallel that can contribute to joint torque. In this way, architectural parameters provide a mechanistic link between the ultrastructural organization of sarcomeres and whole-muscle mechanical capacity. Changes in architecture therefore represent an intermediate scale of adaptation between cellular remodeling and gross hypertrophy.

Resistance training–induced hypertrophy is most consistently associated with increases in mCSA and pennation angle. As myofibrillar material accumulates in parallel, muscle fibers expand radially, and fascicles often rotate to accommodate additional contractile material within the existing connective tissue framework. Increases in pennation angle allow a greater number of fibers, and thus more sarcomeres in parallel, to attach to the tendon, enhancing force-generating capacity even when fascicle length

remains unchanged. Adaptations in fascicle length may also occur, depending on the mechanical environment imposed during training. Increases in fascicle length are commonly interpreted as reflecting the addition of sarcomeres in series and have been reported more frequently under conditions involving sustained stretch or eccentric loading. Such adaptations shift the operating range of sarcomeres along the force–length relationship and may permit greater force production at longer muscle lengths or more extreme joint positions. Importantly, changes in muscle architecture complicate the interpretation of conventional hypertrophy metrics. Anatomical cross-sectional area and muscle thickness represent two-dimensional measurements of a three-dimensional structure and are influenced not only by radial fiber growth, but also by fascicle orientation and length. Straight-line modeling demonstrates that increases in pennation angle alone can increase anatomical cross-sectional area without proportional changes in fascicle length, and that increases in fascicle length can alter cross-sectional area estimates in pennate muscles without corresponding increases in sarcomeres arranged in parallel [34].

Conclusion. In summary, hypertrophy reflects coordinated remodeling across ultrastructural and architectural scales. While increases in muscle size are most consistently associated with radial fiber growth and greater pennation angle, adaptations in fascicle length may occur under specific mechanical conditions and alter sarcomere operating ranges. Importantly, changes in fascicle orientation and length can influence common hypertrophy metrics independently of true increases in sarcomeres arranged in parallel. The presence of fascicle curvature and regional architectural heterogeneity further limits the interpretability of simplified geometric models and underlines the need

for measures across a muscle. Together, these factors highlight the need to consider muscle architecture when interpreting hypertrophic adaptations and relating structural changes to functional outcomes.

Mechanisms of Mechanical Overload-Induced Skeletal Muscle Hypertrophy

Elucidating the mechanisms underlying skeletal muscle hypertrophy is inherently challenging, as adaptation emerges from coordinated processes operating across multiple biological scales. Certain factors act as permissive conditions that enable growth, whereas others may be necessary or sufficient only within specific physiological contexts. Consequently, identifying when and at what level a given mechanism exerts influence is difficult, particularly because many processes interact nonlinearly and may amplify or constrain hypertrophy only after foundational requirements are met. This complexity is further compounded by the likelihood that some mechanisms contribute primarily under specific loading conditions, training histories, or metabolic states rather than serving as universal drivers. As such, hypertrophy cannot be attributed to a single pathway, but instead reflects the integration of mechanical, molecular, and structural processes over time.

Mechanical Tension as the Primary Driver. Mechanical tension is widely regarded as the primary stimulus for resistance training–induced hypertrophy. Experimental work in animal models demonstrates that increases in muscle tension produce graded, dose-dependent activation of anabolic signaling pathways, supporting a causal role for tension

[38]. At the cellular level, forces generated by actin–myosin interactions are transmitted longitudinally and laterally through myofibrils, cytoskeletal networks, the sarcolemma, and the extracellular matrix, forming a continuous mechanical pathway from the sarcomere to the extracellular environment.

Mechanotransduction refers to the process by which these mechanical forces are converted into biochemical signals. Several structural elements within skeletal muscle are well positioned to sense mechanical deformation, including costameres, integrin-associated adhesion complexes, focal adhesion kinase (FAK), Z-disk–associated proteins, and cytoskeletal linkages that connect myofibrils to the nucleus [39, 40]. Mechanical loading deforms these structures, leading to activation of intracellular signaling cascades that regulate gene expression, ribosome biogenesis, and protein synthesis. Mechanical loading has been shown to activate mTORC1 through mechanisms that do not require Akt phosphorylation, implicating alternative mechanosensitive inputs [40, 41]. Phosphatidic acid has been proposed as one such mediator, with experimental evidence indicating that mechanically induced increases in phosphatidic acid content can directly stimulate mTORC1 activity via binding to the FKBP12-rapamycin binding domain of mTOR [42]. While the precise contribution of phosphatidic acid in vivo remains under investigation, these findings support the concept that mechanical deformation of membranes and cytoskeletal structures can generate lipid-based signals that converge on anabolic pathways. Together, these observations support a model in which mechanical strain at the sarcomere and cytoskeletal level serves as the initiating event for hypertrophic signaling, with other inputs acting permissively or modulatory once mechanical requirements are met.

Anabolic Signaling. Mechanical overload initiates a coordinated signaling response that supports both the acute rise in protein synthesis and the longer-term expansion of translational capacity. Central to this response is mTORC1, which integrates mechanical inputs with nutrient and growth factor signals to regulate translation initiation and broader anabolic programming [41]. Importantly, genetic mouse models indicate that mTORC1 is required for full mechanically induced hypertrophy, reinforcing that this pathway is not simply correlated with growth but functionally necessary in overload contexts [43]. When activated, mTORC1 phosphorylates canonical substrates including ribosomal protein S6 kinase beta-1 (S6K1) and eukaryotic translation initiation factor 4E-binding protein 1 (4E-BP1) [12], thereby increasing translational efficiency and supporting net protein accretion within the myofiber. Mechanical loading can engage mTORC1 through mechanisms that are at least partially separable from classic insulin or growth factor signaling. In rodent muscle, mechanical stimulation activates mTOR signaling even when upstream PI3K signaling is not required, supporting a mechanically sensitive control node that is distinct from canonical Akt-mediated regulation [44].

Transcriptional and Translational Capacity. Downstream of mTORC1, mechanical overload promotes not only translation initiation but also the biogenesis of the translational apparatus itself. Mechanical loading rapidly triggers mTOR-dependent ribosomal DNA (rDNA) transcription and chromatin remodeling that precede detectable hypertrophy [45]. Time-course studies in overload models and following resistance exercise demonstrate coordinated induction of c-Myc, Pol I–associated factors, ribosome biogenesis genes, and broader transcriptional shifts that occur before measurable growth,

consistent with an early capacity-building phase that enables subsequent accretion of contractile proteins [46, 47].

Mechanical overload has also been shown to increase skeletal muscle ribosome content [48, 49], as typically assessed using UV A260 RNA concentrations divided by muscle wet weight; notably, this technique is robust and has been validated [50]. Ribosomes serve as the primary machinery for protein synthesis, and their abundance determines the ceiling for translational output [51]. Elevations in muscle RNA content following resistance training may therefore reflect the need to expand the translational machinery required to sustain hypertrophy [52]. While counterevidence exists in certain contexts [53, 54], the preponderance of evidence supports a role for ribosomal capacity in preceding and correlating with hypertrophy or muscle retention, suggesting it may serve as a useful surrogate marker in future work [48, 49, 51]. Ribosome biogenesis is a critical step in driving growth, though skeletal muscle hypertrophy is also dependent on other mechanisms (mTORC1 and increased translational efficiency) and signals (e.g., mRNAs) that dictate when and how translational capacity is utilized.

Satellite Cells and Myonuclear Domain Theory. Beyond the molecular machinery governing protein synthesis, skeletal muscle hypertrophy is constrained by the transcriptional capacity of the fiber itself. Muscle fibers are long, multinucleated, and post-mitotic, and thus remodel through expansion rather than division. Satellite cells, which reside between the sarcolemma and basal lamina, play a key role in this process. In response to exercise-induced mechanical and metabolic stress, satellite cells become activated, proliferate, and fuse with existing fibers, contributing additional myonuclei [55].

While short-term hypertrophy may occur in the absence of satellite cell contribution, as demonstrated in adult mice following short-duration synergist ablation [56], longer-term and more physiologically relevant loading paradigms consistently implicate satellite cells in sustained hypertrophic responses [57, 58]. The myonuclear domain theory proposes that each myonucleus governs gene expression over a finite cytoplasmic volume, such that additional nuclei may be required as fibers enlarge to maintain transcriptional support [59]. Although the precise limits of this domain and the absolute necessity of myonuclear addition remain debated, satellite cell activity is strongly associated with long-term hypertrophy and structural remodeling, particularly under conditions of prolonged or repeated mechanical overload.

Conclusion. Skeletal muscle hypertrophy arises from the integration of mechanical, molecular, and cellular processes that collectively enable the fiber to remodel in response to repeated loading. Mechanical tension experienced at the level of the sarcomere and cytoskeleton is converted into biochemical signals through mechanotransduction pathways, initiating intracellular cascades that regulate protein synthesis, gene expression, and structural remodeling. Anabolic signaling pathways, including mTORC1, coordinate acute translational responses with longer-term expansion of translational capacity through ribosome biogenesis. Hypertrophy therefore depends not solely on increased protein synthesis, but on coordinated regulation of transcription, translation, and cellular architecture. Satellite cell activation and myonuclear addition augment transcriptional capacity, while increases in ribosome content raise the ceiling for protein production. Together, these systems form an integrated network that allows skeletal

muscle to adapt to mechanical demands over time. This mechanistic framework provides the biological context for understanding how resistance training variables, including the mechanical environment experienced by muscle fibers, may shape the magnitude and nature of hypertrophic adaptation.

Resistance Training Variables and Hypertrophy

There are many resistance training variables that can be manipulated to influence hypertrophy outcomes. These mainly include volume, frequency, proximity to failure, load, rest intervals, repetition tempo, progression methods, exercise order, exercise selection, and range of motion. Some variables appear to exert stronger or more consistent effects, whereas others allow for a wide range of flexibility depending on context and preference.

Training Volume. Volume, defined as the number of sets performed close to failure for a given muscle group, is one of the most robust predictors of muscle growth. In a meta-analysis by Pelland et al. [60], "fractional sets" were used to standardize training volume, where a direct set for a muscle group counts as one set and an indirect set counts as 0.5 of a set. Results underlined that while performing more fractional sets generally produces greater hypertrophy, the effect follows a pattern of diminishing returns; specifically, the steepest and most efficient gains occur in the range of about 5–10 fractional sets per week, efficiency is intermediate from roughly 11–18 sets, and progressively lower beyond approximately 19 sets per week. Thus, increasing volume from moderate to high levels produces only modest additional hypertrophy on average, and beyond a certain threshold extra sets contribute little to no benefit.

Training Frequency. Frequency, or how often a muscle is trained, is another important programming variable. Frequency can be viewed both to distribute more total volume across the week and as a lever to manipulate at a given weekly dose. Meta-regression work on weekly volume and frequency shows a small positive hypertrophic effect of training twice per week compared with once, but little evidence for further benefit beyond this when total weekly volume is held constant [60]. Because there is likely a threshold for the anabolic stimulus in a single session, the need for higher frequency generally follows from total weekly training dose.

Proximity to Failure. Proximity to failure is another key determinant of hypertrophy. Higher proximities to failure help ensure that high-threshold motor units are recruited and sufficiently stimulated. Evidence indicates that sets do not need to reach momentary concentric failure to be effective, but they must be performed close to failure to generate an efficient strong growth stimulus [61, 62]. The extent to which this principle varies in multi-joint movements, where some synergist muscles may be trained farther from failure, remains unclear. There is also emerging evidence suggesting an inverse relationship whereby lower training volumes may require closer proximity to failure to maximize adaptations [63]. Overall, current evidence indicates that performing sets with enough proximity to failure is requisite for growth; how proximity to failure interacts with volume and frequency needs further investigation.

Load. Load is another modifiable variable important in resistance training prescription. A large body of evidence shows that hypertrophy is similar across a wide range of repetition schemes [64]. However, there are both physiological and practical

upper and lower bounds to this flexibility. At the heavy end of the spectrum, the hypertrophic effectiveness of each set diminishes as the load approaches a one-repetition maximum [65], and continued reductions in per-set effectiveness may persist down to approximately three repetitions, although evidence here is mixed [66-69]. A conservative lower bound of around five repetitions per set is therefore a practical guideline for maintaining effectiveness. At the lighter end, comparable motor unit recruitment and similar hypertrophy can be achieved when sets are performed close to failure, even with up to 30–50 repetitions. However, at very high repetition ranges (≥60 repetitions) the effectiveness of sets likely declines. Moreover, the ability to accurately gauge proximity to failure decreases beyond about 12 repetitions, making it harder to prescribe a specific repetitions-in-reserve target [70]. Taking both ends of the spectrum into account, a practical recommendation is to use loads that allow roughly 5–15 repetitions per set, while the broader range of 5–35 repetitions per set preserves flexibility for accommodating different populations and limitations.

Rest Intervals Between Sets. Rest intervals are another important and modifiable variable in resistance training. Limited evidence and mechanistic rationale suggest that per-set effectiveness declines as rest between sets is reduced, since adequate time is needed to efficiently recruit and stimulate growth-prone higher-threshold motor units. However, within a practical range of 2 to 3 minutes, rest intervals appear to produce similar hypertrophy outcomes, with some evidence suggesting that longer rest periods may be more effective for lower-body training [71]. Intensity or density techniques can be viewed as a subcategory of rest-period manipulation because they typically involve

shortening or eliminating rest. In line with findings on rest intervals, per-set effectiveness tends to decrease as rest periods shorten. For example, drop sets, which involve no rest between successive bouts, provide a way to increase the density of the training stimulus within a limited time frame. Thus, while a minimum rest threshold is necessary to maximize per-set stimulus, manipulating rest can be a strategy for increasing training density when time is constrained.

Other Training Variables. When it comes to other practical training variables, factors such as repetition tempo, progression method, and exercise order are generally lower on the priority list and offer greater flexibility. In contrast, variables like performing enough sets close to failure represent clear thresholds that must be met for hypertrophy to occur. Together, these training variables interact to shape the adaptive landscape, with some serving as essential prerequisites and others acting as adjustable tools that can be tailored to the lifter or the specific context. One important variable not yet mentioned is exercise selection and range of motion for a given exercise.

Conclusion. Resistance training variables shape the magnitude and efficiency of the hypertrophic stimulus by influencing motor unit recruitment, mechanical tension exposure, and recovery capacity. Among these variables, weekly training volume performed sufficiently close to failure emerges as one of the most consistent predictors of muscle growth, though its effects follow a pattern of diminishing returns. Frequency primarily serves to distribute volume in a manner that supports recovery and maintains stimulus quality, while proximity to failure ensures adequate recruitment of higher-threshold motor units. Load can vary across a wide spectrum provided sets are performed

near failure, and rest intervals within practical ranges appear to allow flexibility without large differences in hypertrophic outcomes. Other programming factors, including tempo, progression methods, and exercise order, offer additional flexibility but are generally secondary to meeting fundamental thresholds of volume and effort. Together, these variables interact to define the overall mechanical and metabolic environment experienced by muscle fibers. While much of the hypertrophy literature has focused on how much stimulus is applied, increasing attention has shifted toward how that stimulus is distributed within a movement. This distinction introduces exercise selection and range of motion as variables that may influence not only the quantity of tension applied, but the muscle lengths and regions at which that tension is experienced, thereby providing a mechanistic bridge to the next section.

Range of Motion: Biomechanical and Physiological Considerations

Understanding how range of motion influences skeletal muscle hypertrophy is challenging because muscle force production and adaptation emerge from the interaction of multiple biomechanical, neural, and cellular processes operating simultaneously across scales. Muscle contributions to movement are shaped by anatomical constraints, joint mechanics, neural control strategies, and intracellular mechanosensing, all of which vary with joint position and loading conditions. Consequently, determining when and how a given muscle experiences meaningful mechanical stimulus is nontrivial, particularly in multi-joint tasks where force sharing, activation strategies, and operating lengths are not

fixed. Within this broader optimization problem, muscle length represents a key, but not isolated, determinant of mechanical tension and signaling.

Muscle Action, Muscle Activation, and Biomechanical Constraints. At the macro level a well-established biomechanical constraint relevant to exercise selection involves biarticular muscles that span two joints and act in opposing directions. During lower-body pressing movements, for example, the RF lengthens at the hip while shortening at the knee during the concentric phase. If fully activated, it would oppose its own action at one of the joints. As a result, the nervous system often recruits less, which may help explain why several studies report reduced RF hypertrophy during compound pressing exercises [10, 72]. Similar constraints apply to the hamstrings during lower-body pressing and to the long head of the triceps during upper-body pressing movements [73-75].

However, muscle contribution to movement is not determined solely by anatomy. Multiple activation strategies can achieve the same joint-level outcome, a phenomenon commonly referred to as the redundancy problem [76]. Numerous optimization-based hypotheses have been proposed to explain how the nervous system resolves this redundancy [77]. In contrast, the principle of abundance suggests that the central nervous system does not compute a single optimal solution but instead organizes muscle synergies that stabilize task-relevant variables [78]. While no single framework fully accounts for muscle activation patterns across tasks, these perspectives highlight that activation is context dependent and not uniformly distributed across muscles or joint positions. Continuing at the macro level, joint biomechanics further shape how mechanical stress is distributed across range of motion. Muscle moment arms vary with

joint angle, altering the torque a muscle can generate for a given level of force. External moment arms imposed by exercise equipment interact with internal moment arms and as a result the joint angles at which a muscle experiences the greatest relative mechanical challenge depend on both musculoskeletal geometry and external loading characteristics.

Muscle Architecture and Operating Lengths In Vivo. The relationship between muscle length and tension provides a foundational framework for understanding how range of motion may influence hypertrophy. At the sarcomere level, force capacity depends on the degree of actin–myosin overlap. Active force is greatest near optimal sarcomere length, declines on the ascending limb when sarcomeres are overly shortened, and decreases on the descending limb when overlap becomes insufficient [79]. In addition to active force, passive tension rises at longer muscle lengths due largely to elastic elements such as titin and connective tissue structures.

Conclusion. Together, the combined effects of length–tension mechanics, musculoskeletal architecture, joint biomechanics, neural excitation, and cellular mechanotransduction create a complex landscape in which exercise selection and range of motion influence both activation patterns and the internal mechanical environment of muscle fibers. Ultimately, hypertrophy reflects how these mechanical and neural processes are transduced into intracellular signaling within the muscle fiber. At present, the only definitive way to determine which range of motion produces selective or superior hypertrophy in a given exercise is through longitudinal studies directly measuring muscle accretion over time.

Evidence for Length-Dependent Hypertrophy

Range of motion and particularly training at long muscle lengths has recently received attention as a variable with unique hypertrophic potential. Emerging evidence suggests that training at longer muscle lengths, either with exercising a biarticular muscle in a more lengthened position or using partial repetitions in a more lengthened position, may provide a hypertrophic advantage.

Biarticular Muscles Trained at Different Static Positions. Several studies have compared biarticular muscles trained at longer versus shorter muscle lengths. For example, seated hamstring curls, which place the hamstrings in a more lengthened position due to hip flexion, have produced greater hypertrophy than lying or Nordic hamstring curls after 12 weeks of training [2, 80]. Similarly, the RF, which spans both the hip and knee, demonstrated greater growth when trained under conditions of increased hip extension, such as leaning back, which lengthens the muscle [3]. The gastrocnemius, a biarticular muscle crossing the knee and ankle, also exhibited greater hypertrophy when trained with the knee extended (straight-leg) compared to the bent-leg condition [4]. Although findings for the triceps brachii are more mixed, the most rigorous study design and measurement methods to date showed that elbow extensions performed in the overhead position, relative to a neutral humerus position, produced greater growth [81]. Collectively, these results suggest that training biarticular muscles in more lengthened static positions generally leads to superior hypertrophic adaptations compared to training at shorter lengths. Future work will build on this evidence to confirm whether this holds true for all biarticular muscles.

Range of Motion and Resistance Challenge. With respect to range of motion and the magnitude of the resistance challenge, the observed effects are generally modest; however, the overall body of evidence suggests a small benefit in favor of applying load at longer muscle lengths across many contexts. In the calves, emphasizing the lengthened or initial portion of a calf raise consistently produces greater hypertrophy than training with shortened partial or full range of motion [5], and has even demonstrated slight superiority over full range of motion training performed beyond momentary concentric failure [82]. Quadriceps hypertrophy is also greater when training through a larger range of motion in squats (90 vs. 50 degrees of knee flexion) [6] and when performing partial repetitions in the lengthened position compared to full range of motion leg extensions [83]. However, applying tension at approximately 90 degrees of knee flexion appears sufficient to maximize quadriceps hypertrophy during squats and leg presses, though not for the gluteus and adductor muscle groups [10, 84]. Evidence in the elbow flexors similarly trends toward an advantage for the lengthened position, as preacher curls performed in the first half of the range of motion produce greater hypertrophy, particularly in the distal region of the elbow flexors [7, 85]. Overall, findings related to range of motion differences indicate a small but consistent benefit to emphasizing training in more lengthened muscle positions. Future work should determine whether this effect generalizes across muscles or is muscle- or region-specific.

Regional Hypertrophy. Several studies indicate that hypertrophy can vary by region within a muscle, suggesting that strain distribution and regional loading patterns may influence local growth responses. However, this evidence base remains limited, and

strong conclusions should be avoided. A recent meta-analysis highlights the uncertainty in the current literature [86]. More broadly, these findings emphasize the need to clarify underlying mechanisms, including the roles of passive tension, fascicle lengthening, regional strain distribution, and their interaction with mechanotransduction pathways.

Conclusion. Taken together, the literature suggests that hypertrophy is generally enhanced when resistance training emphasizes a more lengthened portion of a muscle's range of motion. However, effects may not be uniform across muscles or regions, and outcomes may depend on muscle architecture, joint mechanics, resistance profile, and the degree to which conventional full range training already exposes the muscle to high tension at long lengths. These uncertainties underscore the need for controlled studies in trained individuals using comprehensive imaging and molecular approaches to clarify the mechanisms and muscle-specific nature of length-dependent hypertrophy.

Introduction to the Project

The present dissertation was designed to address the literature gap proposed in the preceding paragraphs by integrating whole-muscle and cellular analyses within controlled range of motion interventions in resistance-trained individuals. Specifically, the laboratory and collaborators will perform an acute and chronic intervention in resistance-trained men using unilateral within-subject designs to address these gaps. In Experiment 1 (acute bout), participants will perform one bout of unilateral leg extension exercise whereby one leg is assigned full range of motion (FULL; week 1 or 2 bout), and the contralateral leg (week 2 or 1 bout) is assigned LP training with four sets to concentric failure. VL biopsies

will be collected PRE as well as at 0h POST, 3h POST, and 24h POST. Outcomes will include global mRNA assessments (i.e., the protein-coding transcriptome) as well as phosphorylated mTORC1 and Hippo signaling protein targets. This study will be the first human investigation to examine range of motion resistance training effects on molecular outcomes in trained individuals. Experiment 2 will involve an independent cohort of participants who will perform LP range of motion training for 8 weeks (2 days per week) whereby one leg is assigned FULL and the contralateral leg is assigned LP across three exercises including leg press, leg extension, and lying leg curl. Again, this study will be the first human investigation to examine range of motion resistance training effects using MRI-derived mCSA or VL biopsies to assess fCSA, satellite cell number, and total RNA content in trained individuals.

Chapter 3: Methods

Participants and Ethical Approval

All study procedures were conducted in accordance with the Declaration of Helsinki, and all participants provided written informed consent prior to enrollment. Inclusion criteria for both experiments required: i) a minimum of 3 years of consistent resistance training experience with at least two lower-body sessions per week; ii) no lower-extremity musculoskeletal injury within the preceding 6 months; and iii) no contraindications to percutaneous skeletal muscle biopsies. Experiment 2 also contained the stipulation that no contraindications existed for MRI scanning. In Experiment 1, 8 resistance-trained males between the ages of 18–35 years old were recruited from the local Belton, TX area following approval by the University of Mary Hardin-Baylor's IRB. In Experiment 2, 18 resistance-trained males between the ages of 18–35 years were recruited from the local Auburn, AL area (IRB: STUDY00000282, Auburn University).

Experiment 1

Experiment 1 employed a within-subject crossover design in which participants completed two unilateral leg extension exercise bouts separated by one week. Participants first completed an informed consent and phenotyping visit including health history and a dual-energy x-ray absorptiometry (DXA) scan for body composition phenotyping purposes. A separate session established 10RM loads for each condition, conducted 3–5 days prior to the first training bout. Each leg was then randomly assigned to either FULL (100–0° knee flexion) or LP (100–50° knee flexion), and bouts were completed in counterbalanced order.

Participants were block randomized by limb to counterbalance for limb dominance, and exercise bouts were performed on a unilateral weight stack leg extension machine. Participants arrived in an approximately 12-hour fasted state between 0800 and 1200 for each visit. Each bout consisted of a standardized warm-up set followed by four sets to concentric failure using a 10-repetition maximum (10RM) load for each respective condition with 2 minutes of rest between sets. Vastus lateralis (VL) biopsies were obtained from the mid-thigh prior to (PRE) and immediately (0h), 3 hours (3h), and 24 hours (24h) after exercise. Participants were instructed to avoid lower-body exercise for at least 48 hours before each visit and to maintain similar dietary habits in the 48 hours prior to and the day of each bout.

Muscle Biopsies. Mid-thigh VL biopsies were obtained using a 14-gauge needle with suction under aseptic conditions as previously described [87]. Three passes were collected yielding approximately 30 mg of tissue per biopsy. Tissue allocated was rapidly cleaned of blood, fat, and connective tissue, placed in cryogenic vials, flash frozen in liquid nitrogen, and stored at −80°C.

Transcriptomics. RNA was isolated from VL tissue using Trizol and shipped on dry ice to a commercial laboratory for transcriptome-wide analysis using the Clariom S Assay Human mRNA array (North American Genomics; Decatur, GA, USA). Raw .CEL files were analyzed using Transcriptome Analysis Console (TAC) v4.0.2 (Thermo Fisher; Waltham, MA, USA) with the H. sapiens genome for reference annotations. Two analyses were conducted. First, pairwise comparisons identified mRNAs altered from PRE within each

bout; targets were considered significant at ≥1.5-fold change and nominal $p < 0.01$. Second, 2×2 repeated measures ANOVAs with the eBayes correction were performed to identify mRNAs that differed between bouts over time, with the same fold-change and $p < 0.01$ thresholds applied to the interaction. Bioinformatics analyses on resulting gene lists were performed using PANTHER v17.0 as previously described [88].

Western Blotting. Muscle tissue was lysed using general cell lysis buffer (Cell Signaling Technology; cat. no. 9803) with tight-fitting pestles. Total protein was quantified using a BCA protein assay kit (cat. no. A55864; Thermo Fisher) and spectrophotometer (Agilent Biotek Synergy H1, Thermo Fisher). Lysates were prepared for SDS-PAGE with 4× Laemmli buffer at equal protein concentrations (1 µg/µL) and 15 µL was loaded onto 4–15% Criterion TGX Stain-Free gels (Bio-Rad; Hercules, CA, USA). Electrophoresis was run at 200 V for 45–50 minutes. Proteins were transferred to PVDF membranes (Bio-Rad) for 2 hours at 200 mA, Ponceau stained and imaged (ChemiDoc Touch, Bio-Rad), and then blocked for 1 hour at room temperature with 5% nonfat milk powder in Tris-buffered saline with 0.1% Tween-20 (TBST, VWR International; Radnor, PA, USA), and incubated overnight at 4°C with primary antibodies (1:1000 in TBST with 5% bovine serum albumin) from a commercial vendor (Cell Signaling Technology; Danvers, MA, USA). These antibodies targeted phosphorylated (p-) LATS1 (Thr1079) (cat. no. 8654), p-YAP (Ser127) (cat. no. 4911), p-TAZ (Ser89) (cat. no. 4911), p-mTOR (Ser2448) (cat. no. 5536), p-p70S6K (Thr389) (cat. no. 9234), and p-rpS6 (Ser235/236) (cat. no. 4858). The following day, membranes were washed for 15 minutes in TBST and incubated with a horseradish peroxidase-conjugated anti-rabbit secondary antibodies diluted 1:2000 in TBST with 5% BSA (cat. no.

7074; Cell Signaling Technology) at room temperature for 1 hour. Membrane development was performed using an enhanced chemiluminescent reagent (cat. no. ELLUF0100, Millipore Sigma; Burlington, MA, USA), and band densitometry was performed using a gel documentation system and associated densitometry software (ChemiDoc Touch, Bio-Rad). Band densities for phosphorylated targets were normalized to corresponding Ponceau densities as we have previously performed with acute bout settings [89], and fold-change values were derived relative to the aggregate PRE mean of the FULL condition.

Experiment 2

Chronic Experimental Design. Experiment 2 employed a within-subject contralateral limb design over 8 weeks using the 45-degree leg press, seated knee extension, and lying knee flexion exercises. One leg was assigned to FULL and the contralateral leg to LP for the duration of the intervention, and again participants were block randomized by limb to counterbalance for limb dominance. Participants first completed an informed consent and phenotyping visit including health history screening, body composition assessment using bioelectrical impedance spectroscopy (SFB7, Impedimed; Carlsbad, CA, USA) and familiarization with the range of motion for each condition on the leg press. Three to five days thereafter, participants attended the Auburn University MRI Research Center in a greater than 4-hour fasted state for pre-intervention lower-body MRI scanning. Participants were instructed to cease resistance training 72 hours prior to the initial MRI scan. One to two days following the MRI scan, pre-intervention bilateral VL biopsies were collected. Participants then completed 16 supervised resistance training sessions across 8 weeks (2 days/week). Eighty-seven to 96 hours after the final

training session, participants returned for post-intervention MRI scanning, followed 1 to 2 days later by post-intervention bilateral VL biopsies. Participants were instructed to avoid lower-body resistance training outside of supervised sessions for the duration of the intervention.

Resistance Training Protocol. Exercises were performed in the following order: unilateral leg press (Arsenal Strength Reloaded Linear Leg Press; Arsenal Strength, Lenoir City, TN), unilateral leg extension, and lying leg curl (Life Fitness Signature Series; Life Fitness, Franklin Park, IL). A slant board (20 Degree Slant Board; SquatWedgiez) was adhered to the footplate of the leg press using hook-and-loop tape (Melsan 4x6 Inch Hook and Loop Tape Heavy Duty; Melsan) to allow full knee flexion to be achieved without heel elevation. The seatback of the leg press was positioned one setting from fully reclined for all participants. For the leg press, both conditions performed the exercise to maximal knee flexion, with each participant able to touch their calf to their hamstring at the bottom of each repetition. FULL condition participants completed approximately double the ROM of the LP condition but did not fully lock out the knee at the top of the movement to prevent offloading. LP participants extended to approximately the midpoint of the full ROM. During the LP condition, a metal device was held by a staff member with extensive resistance training supervision experience at the targeted position to provide an audible cue when participants pressed the metal sled plate to the assigned LP extension endpoint. Unilateral leg extension was performed through either FULL (100–0° knee flexion) or LP (100–50° knee flexion) ranges of motion, monitored visually by certified trainers. Lying leg curl was performed through full individualized ROM for FULL and 0–80° knee flexion for LP to

account for greater gastrocnemius involvement in the early portion of the range of motion; the LP endpoint was enforced via a physical block held by a trained researcher. Each repetition was initiated at a controlled tempo and transitioned to maximal intended velocity as fatigue accumulated naturally within the set; this approach was employed to avoid tempo-related biases favoring the lengthened position. Leg press was performed to volitional failure, defined as the point at which the participant believed the next repetition could not be completed or would require compromised form. Leg extension and leg curl were performed to concentric failure, defined as the inability to complete the assigned range of motion. Sets and rest periods were exercise-specific: leg press progressed from 3 sets (sessions 1–9) to 4 sets (sessions 10 onward) with 1.5 minutes of rest between sets, alternating the starting leg each set; leg extension progressed from 3 sets (sessions 1–3) to 4 sets (sessions 4 onward) with 1 minute of rest between sets; and leg curl progressed from 5 sets (sessions 1–5) to 6 sets (sessions 6 onward) with 1 minute of rest between sets. Approximately 2 minutes separated the leg press and leg extension blocks, while the transition from leg extension to leg curl was self-paced.

Leg press kinematics. ROM adherence was confirmed during session 10 of 16, in which participants were fitted with inertial measurement units (IMUs; Noraxon Ultium Motion, Noraxon U.S.A., Scottsdale, AZ) on each shin and thigh to verify that each leg was trained within its assigned range of motion via wireless transmission to myoRESEARCH software (Noraxon U.S.A., Scottsdale, AZ). Raw joint angle data exported from myoRESEARCH were processed in R (version 4.4.1; R Core Team, 2024). Knee and hip flexion signals were each smoothed using a 7-point centered moving average filter prior to

repetition detection. Individual repetitions were identified from peaks in the smoothed knee signal using a minimum peak separation of 0.20 seconds. The first and last repetitions of each set were excluded when four or more repetitions were detected to minimize the influence of transition periods. All processed files were visually inspected to confirm accurate repetition detection. Peak flexion, minimum flexion, and ROM were extracted from each retained repetition and averaged across repetitions within each set, then across sets within each leg.

Magnetic Resonance Imaging. MRI scanning was performed on a 3T SkyraFit system (Siemens, Erlangen, Germany) at the Auburn University MRI Research Center. Participants were positioned prone on the patient table with an approximately 5-minute latency period before scanning. A T1-weighted turbo spin echo pulse sequence was used (repetition time: 1,400 ms; echo time: 23 ms; in-plane resolution: 0.9 × 0.9 mm^2) to obtain transverse image sets spanning the top of the ilium to the patella with a 2-mm slice thickness and no inter-slice gap. All image analysis was performed blinded to training conditions by the same investigator (R.J.B.). DICOM files were preprocessed in OsiriX MD (Pixmeo, Geneva, Switzerland) and imported into 3D Slicer (Brigham and Women's Hospital, Boston, MA), where the polygon tool was used to manually trace VL borders on each image. Image standardization was as follows: i) the most proximal slice was defined as the first axial image in which the gluteal musculature was no longer visible; ii) the most distal slice was defined as 10 slices (2 cm) proximal to the final image in which the RF was no longer visible; iii) five equidistant slices were selected between the proximal and distal

boundaries at both PRE and POST. Total VL mCSA was computed as the sum of mCSA values across the five slices.

Muscle Biopsies. Mid-thigh VL biopsies were obtained using a 5-gauge needle with suction under aseptic conditions as previously described by our laboratory [90]. Approximately 80–140 mg of muscle tissue was excised per biopsy. Tissue allocated for histological analysis was mounted in optimal cutting temperature (OCT) compound, frozen in liquid nitrogen-cooled isopentane, and stored at −80°C. Tissue for molecular analyses was rapidly cleaned of blood, fat, and connective tissue, placed in cryogenic vials, flash frozen in liquid nitrogen, and stored at −80°C.

Immunohistochemistry. Cryosections (12 µm) were cut using a cryostat (Leica Biosystems, Buffalo Grove, IL), adhered to positively charged histological slides, and stored at −80°C until batch processing. All samples from the same participant were processed on the same slide simultaneously. Sections were air-dried for 2 hours at room temperature and fixed in −20°C acetone for 5 minutes. Slides were then incubated with 3% H_2O_2 for 10 minutes, treated with autofluorescence quenching reagent (cat. no. 23007; Biotium, Fremont, CA, USA) for 1 minute and blocked for 1 hour with a solution of 5% goat serum, 2.5% horse serum, and 0.1% Triton-X at room temperature. Thereafter, slides were blocked with a streptavidin and biotin blocking solutions (cat. no. SP-2002; Vector Laboratories; Newark, CA, USA) at room temperature for 15 minutes each, with 5-minute PBS washes occurring between these incubations. Slides were then incubated overnight at 4°C with primary antibody cocktail containing 1:100 rabbit anti-dystrophin IgG (cat. no.

GTX57970; Abcam; Waltham, MA, USA), 1:100 mouse anti-MyHCI IgG2b (clone: BA-D5; Developmental Studies Hybridoma Bank; Iowa City, IA, USA), and 1:20 mouse anti-PAX7 IgG1 (Developmental Studies Hybridoma Bank) + 2.5% horse serum in PBS. The following day, slides were washed four times (5 minutes each) in PBS and incubated for 90 minutes in biotin-SP-conjugated goat anti-mouse IgG1 (1:1,000) (cat. no. 111-065-003; Jackson ImmunoResearch; West Grove, PA, USA) in 2.5% BSA for 90 minutes. This step was followed by three 5-minute PBS washes and a 60-minute incubation with a solution containing 1:500 streptavidin (cat. no. S911; Thermo Fisher Scientific), 1:250 goat anti-mouse IgG2b Alexa Fluor 488 (cat. no. A21141; Thermo Fisher Scientific) and 1:250 goat anti-rabbit IgG Alexa Fluor 647 (cat. no. A21245; Thermo Fisher Scientific) in PBS. Following three 5-minute PBS washes, slides underwent a 20-minute incubation with 1:200 Alexa Fluor 555 tyramide (cat. no. B40955; Thermo Fisher Scientific) in PBS. Following three 5-minute PBS washes nuclei were stained with DAPI (1:10,000; cat. no. D3571; Thermo Fisher Scientific) for 10 minutes, washed twice (5 minutes each) in PBS, and sections were mounted with 1:1 PBS/glycerol. Digital images were acquired at 10× (fCSA) and 20× (nuclei as well as satellite cells) objectives using a fluorescent microscope (Zeiss Axio Imager.M2 with motorized stage). Image analysis was automated using MyoVision v1.0 [91] for fiber type-specific fCSA and myonuclei per fiber. Satellite cells were manually counted by an investigator blinded to training conditions (C.E.) and expressed as number per 100 fibers (DAPI-positive & PAX7-positive cells within the dystrophin border).

Total RNA Content. Approximately 20 mg of muscle tissue was homogenized in Trizol (cat. no. 15596026; ThermoFisher) per manufacturer's instructions. RNA pellets

were reconstituted in 30 µL of diethyl pyrocarbonate (DEPC)-treated water and quantified in duplicate using a NanoDrop Lite spectrophotometer (ThermoFisher). Total RNA content was normalized to input tissue wet weight and expressed as ng RNA per mg tissue, a validated surrogate of muscle ribosome content [50].

Statistical Analysis

All statistical analyses were conducted in R using the lme4 and lmerTest packages. For Experiment 1 western blot outcomes and all Experiment 2 outcomes, a linear mixed-effects model (LMM) was fitted with Condition (FULL vs. LP), Time (PRE vs. POST for Experiment 2; PRE vs. 0h/3h/24h POST for Experiment 1), and their Condition × Time interaction as fixed effects. To account for the contralateral-limb design and repeated measurements, random intercepts were included for participant and for participant-by-condition, reflecting that each participant contributed both a FULL and LP limb measured at multiple points. Estimated marginal means, standard errors, 95% confidence intervals, and planned contrasts were derived using the emmeans package. For Experiment 1 western blot outcomes, follow-up pairwise comparisons between conditions at each timepoint were conducted with Sidak adjustment when a significant Condition × Time interaction was observed. For significant main effects of Time in the absence of a significant Condition × Time interaction, contrasts versus PRE collapsed across conditions were conducted with Sidak adjustment. Statistical significance was set at $\alpha = 0.05$. However, interpretation focused on the magnitude and precision of estimated effects rather than statistical significance alone. Because equivalence margins were not

prespecified, non-significant Condition × Time interactions were interpreted as indicating no clear evidence of a differential response between conditions, rather than formal statistical equivalence. To confirm the ROM manipulation, paired t-tests were used to compare FULL and LP conditions for knee and hip ROM and peak flexion angles at session 10, with each participant contributing one value per condition averaged across sets. Data are presented as estimated marginal means ± SE unless otherwise noted; descriptive characteristics are presented as mean ± SD. For Experiment 1 transcriptomic analyses, the statistical approach is described in the Transcriptomics section above.

Chapter 4: Pending Manuscript

Acute molecular and chronic vastus lateralis adaptations to lengthened partial versus full range of motion resistance training in previously-trained males

Daniel L. Plotkin[1], Dakota R. Tiede[1], Tahran Gotla[1], Jaci Kelly[2], Mathis Rollin[2], Josh Queneua[2], Colin D. Wilborn[3], Marina Meyer-Vega[1], Valeria Robles-Cerdas[1], Adil Bashir[4], Ronald J. Beyers[4], Camila A. Esquivel[1], Christopher B. Mobley[1], Ryan Babl[1], Andreas N. Kavazis[1], Darren T. Beck[1,5], Harsimran S. Baweja[1,5], Christopher G. Vann[6], Paul Swinton[7], Lemuel L. Taylor[3,*],Michael D. Roberts[1,5,*]

Affiliations: [1]School of Kinesiology, Auburn University, Auburn, AL, USA; [2]School of Exercise and Sports Science, University of Mary Hardin-Baylor, Belton, TX, USA; [3]School of Health Professions, University of Mary Hardin-Baylor, Belton, TX, USA; [4]MRI Research Center, Auburn University, Auburn AL, USA; [5]Edward Via College of Osteopathic Medicine-Auburn Campus, Auburn, AL, USA; [6]Duke Molecular Physiology Institute, Duke University School of Medicine, Duke University, Durham, NC, USA; [7] Robert Gordon University, Aberdeen, United Kingdom

*, co-PI/co-correspondence to:

Michael D. Roberts, PhD
Professor
Director, Nutrabolt Applied and Molecular Physiology Laboratory
School of Kinesiology, Auburn University
Auburn AL, USA
E-mail: mdr0024@auburn.edu

Lemuel L. Taylor, PhD
Professor
Director, Director of the Human Performance Laboratory
Doctor of Physical Therapy Program & School of Exercise and Sports Science, University of Mary Hardin-Baylor
Belton, TX, USA
E-mail: ltaylor@umhb.edu

Abstract

This study examined how lengthened partial (LP) versus full range of motion (FULL) lower-body resistance training affects acute post-exercise signaling and chronic hypertrophy and cellular adaptations of the vastus lateralis (VL) muscle in resistance-trained men. Eight men (22±1 years old, 5.6±1.4 years training experience) completed a crossover study whereby VL biopsies were collected pre-exercise and 0, 3, and 24 hours following LP and FULL leg extension bouts for transcriptomic and anabolic signaling analyses (Experiment 1). Another 16 men (26±5 years old; 8.0 ± 4.9 years training experience) completed an 8-week, twice-weekly lower-body intervention using a within-subject contralateral limb design (Experiment 2). One leg was randomly assigned to FULL and the contralateral leg to LP training across three exercises (leg press, leg extension, and lying leg curl). Pre- and post-intervention outcomes included VL muscle cross-sectional area (mCSA) summed across five equidistant MRI-derived transverse and mid-thigh biopsy outcomes. Condition × Time interactions for all outcomes were assessed using linear mixed-effects models. In Experiment 1, both conditions produced similar time-dependent changes in the VL transcriptome and anabolic signaling, but minimal between-protocol interactions. In Experiment 2, VL summed mCSA significantly increased over time (mean change: 9.3 cm^2, 95% CI [6.8, 11.8], P<0.001), but there was no clear evidence of differential change between LP and FULL (LP − FULL change: −1.4 cm^2, 95% CI [−6.1, 3.4], P = 0.640). Additionally, no significant interactions existed for type I fiber CSA (P=0.476), type II fiber CSA (P=0.350), type I fiber myonuclei (P=0.813), type II fiber myonuclei (P=0.589), type I and II satellite cell number (P=0.102 and P=0.797, respectively), or total RNA content

(P=0.537). In conclusion, these data suggest that LP and FULL resistance training when executed within a typical lower body program broadly elicit similar chronic VL responses in previously trained men.

Keywords: resistance training; range of motion; muscle hypertrophy; MRI; satellite cells; transcriptomics

Introduction

Skeletal muscle hypertrophy is a primary adaptation to resistance training and is largely governed by the magnitude, distribution, and characteristics of the mechanical stimulus imposed on muscle fibers [12]. Among the training variables that influence mechanical loading and subsequent hypertrophic outcomes, the range of motion (ROM) through which an exercise is performed has received increasing attention. A growing body of evidence suggests that training at longer muscle lengths, either through positioning biarticular muscles in more lengthened joint configurations or by restricting repetitions to the lengthened portion of the movement arc (i.e., lengthened partial repetitions), may enhance hypertrophic outcomes relative to conventional full ROM training in specific muscles [5, 83].

Evidence for length-dependent hypertrophy in biarticular muscles exists for the hamstrings which experience more growth in hip flexion versus hip neutral positions during seated hamstring curls [2, 80]. Likewise, the rectus femoris demonstrates greater hypertrophy when trained in conditions that increase hip extension and muscle length [3]. Similarly, the gastrocnemius exhibits greater hypertrophy when trained with the knee extended versus flexed [4]. Although the evidence is mixed, the totality of findings suggests that lengthened-biased training produces greater hypertrophy than shortened-biased or full ROM training, at least within isolated comparisons. Importantly, however, many of these comparisons involve full ROM exercises where the resistance challenge is predominantly shortened-dominant, such as the calf raise and leg extension performed on conventional machines [5, 83]. While these findings are broadly consistent with a length-

dependent hypertrophy advantage, several important limitations temper strong conclusions. Whether these findings generalize across different resistance profiles, whether a greater lengthened challenge confers proportionally greater hypertrophy, and whether such effects would persist within the context of a full training program incorporating exercises that emphasize a range of muscle lengths remain to be established.

Despite the growing ROM literature, several key gaps remain. First, a large majority of studies have been conducted in untrained individuals, with few controlled trials in resistance-trained populations. Second, most studies have used ultrasound-derived muscle thickness at one or two sites rather than MRI-based assessment of muscle cross-sectional area (mCSA) across the length of the muscle, which provides a more comprehensive characterization of the hypertrophic response. Third, no prior human work has combined whole-muscle MRI with biopsy-derived measures of fiber type-specific CSA (fCSA), satellite cell content, myonuclear number, and RNA content (a surrogate of ribosome content) when comparing ROM protocols, leaving the cellular mechanisms underlying any potential differential responses uncharacterized. Finally, the acute transcriptomic and anabolic signaling responses to LP versus FULL resistance exercise have not been described.

Therefore, the purpose of this investigation was twofold. Experiment 1 examined whether an acute bout of LP versus FULL unilateral leg extension exercise produced differential transcriptomic and anabolic signaling responses in the VL of resistance-trained men. Experiment 2 examined whether 8 weeks of LP versus FULL lower-body resistance

training produced differential VL hypertrophy and cellular adaptations in a separate cohort of resistance-trained men, using MRI-derived mCSA across five equidistant slices and biopsy-derived measures of fCSA, SC number, myonuclear number, and total RNA content.

Methods

Participants and Ethical Approval

All study procedures were conducted in accordance with the Declaration of Helsinki, and all participants provided written informed consent prior to enrollment. Inclusion criteria for both experiments required: i) a minimum of 3 years of consistent resistance training experience with at least two lower-body sessions per week; ii) no lower-extremity musculoskeletal injury within the preceding 6 months; and iii) no contraindications to percutaneous skeletal muscle biopsies. Experiment 2 also contained the stipulation that no contraindications existed for MRI scanning. In Experiment 1, 8 resistance-trained males between the ages of 18–35 years old were recruited from the local Belton, TX area (IRB protocol no. LT81725). In Experiment 2, 18 resistance-trained males between the ages of 18–35 years were recruited from the local Auburn, AL area (IRB protocol no. STUDY00000282, Auburn University). An overview of both experiments is presented in Figure 1.

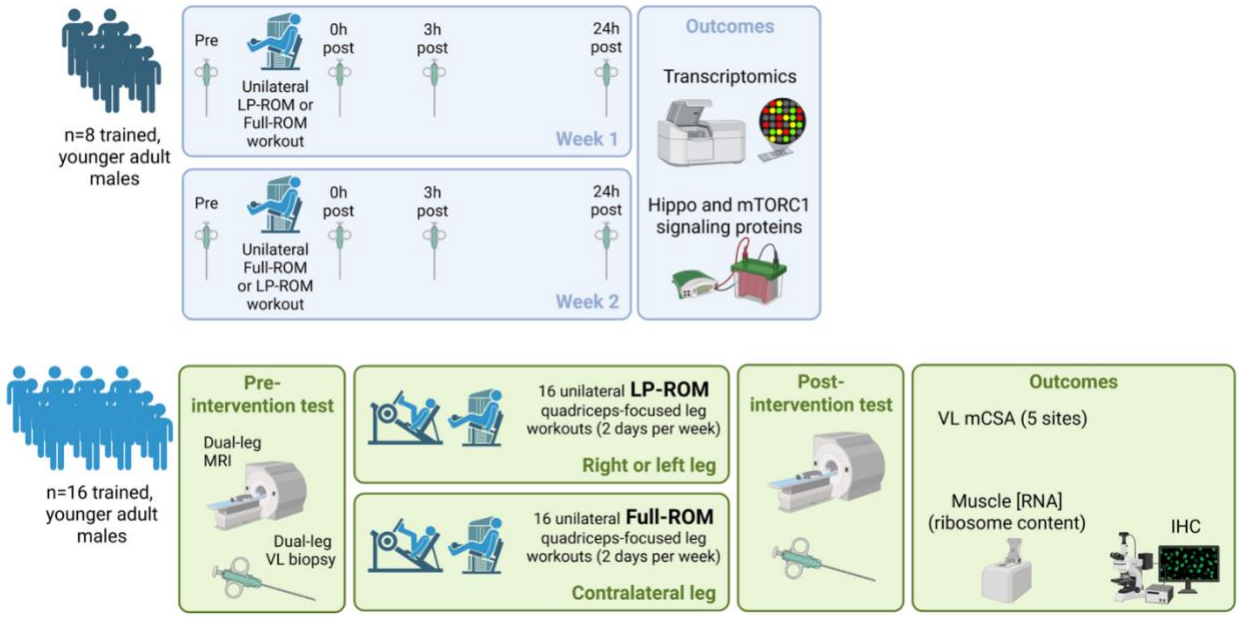

FIGURE 1. Study design overview. The upper panel depicts the Experiment 1 (acute) design, in which resistance-trained men completed a within-subject crossover with one leg performing LP-ROM and the contralateral leg performing Full-ROM unilateral leg extension across two separate weeks (counterbalanced order). VL biopsies were collected at PRE, 0h, 3h, and 24h post-exercise for transcriptomic and anabolic signaling analyses. The lower panel depicts the Experiment 2 (chronic) design, in which a separate cohort of resistance-trained men performed 16 unilateral LP-ROM (one leg) and Full-ROM (contralateral leg) quadriceps-focused workouts over 8 weeks (2 days/week), with pre- and post-intervention bilateral MRI and VL biopsy assessments. Abbreviations: Full-ROM, full range of motion; LP-ROM, lengthened partial range of motion; IHC, immunohistochemistry mCSA, muscle cross-sectional area; VL, vastus lateralis.

Experiment 1

Experiment 1 employed a within-subject crossover design in which participants completed two unilateral leg extension exercise bouts separated by one week. Participants first completed an informed consent and phenotyping visit including health history and a dual-energy x-ray absorptiometry (DXA) scan for body composition phenotyping purposes. A separate session established 10RM loads for each condition, conducted 3–5 days prior to the first training bout. Each leg was then randomly assigned to either FULL (100–0° knee flexion) or LP (100–50° knee flexion), and bouts were completed in counterbalanced order.

Participants were block randomized by limb to counterbalance for limb dominance, and exercise bouts were performed on a unilateral weight stack leg extension machine. Participants arrived in an approximately 12-hour fasted state between 0800 and 1200 for each visit. Each bout consisted of a standardized warm-up set followed by four sets to concentric failure using a 10-repetition maximum (10RM) load for each respective condition with 2 minutes of rest between sets. Vastus lateralis (VL) biopsies were obtained from the mid-thigh prior to (PRE) and immediately (0h), 3 hours (3h), and 24 hours (24h) after exercise. Participants were instructed to avoid lower-body exercise for at least 48 hours before each visit and to maintain similar dietary habits in the 48 hours prior to and the day of each bout.

Muscle Biopsies. Mid-thigh VL biopsies were obtained using a 14-gauge needle with suction under aseptic conditions as previously described [87]. Three passes were collected yielding approximately 30 mg of tissue per biopsy. Tissue allocated was rapidly cleaned of blood, fat, and connective tissue, placed in cryogenic vials, flash frozen in liquid nitrogen, and stored at −80°C.

Transcriptomics. RNA was isolated from VL tissue using Trizol and shipped on dry ice to a commercial laboratory for transcriptome-wide analysis using the Clariom S Assay Human mRNA array (North American Genomics; Decatur, GA, USA). Raw .CEL files were analyzed using Transcriptome Analysis Console (TAC) v4.0.2 (Thermo Fisher; Waltham, MA, USA) with the H. sapiens genome for reference annotations. Two analyses were conducted. First, pairwise comparisons identified mRNAs altered from PRE within each

bout; targets were considered significant at ≥1.5-fold change and nominal $P < 0.01$. Second, 2×2 repeated measures ANOVAs with the eBayes correction were performed to identify mRNAs that differed between bouts over time, with the same fold-change and $P < 0.01$ thresholds applied to the interaction. Bioinformatics analyses on resulting gene lists were performed using PANTHER v17.0 as previously described [88], whereby predicted pathways were considered significant if pathway FDR values were less than 0.05. Note, pathways with less than 20 genes and/or not related to skeletal muscle physiology were manually filtered out.

Western Blotting. Muscle tissue was lysed using general cell lysis buffer (Cell Signaling Technology; cat. no. 9803) with tight-fitting pestles. Total protein was quantified using a BCA protein assay kit (cat. no. A55864; Thermo Fisher) and spectrophotometer (Agilent Biotek Synergy H1, Thermo Fisher). Lysates were prepared for SDS-PAGE with 4× Laemmli buffer at equal protein concentrations (1 µg/µL) and 15 µL was loaded onto 4–15% Criterion TGX Stain-Free gels (Bio-Rad; Hercules, CA, USA). Electrophoresis was run at 200 V for 45–50 minutes. Proteins were transferred to PVDF membranes (Bio-Rad) for 2 hours at 200 mA, Ponceau stained and imaged (ChemiDoc Touch, Bio-Rad), and then blocked for 1 hour at room temperature with 5% nonfat milk powder in Tris-buffered saline with 0.1% Tween-20 (TBST, VWR International; Radnor, PA, USA), and incubated overnight at 4°C with primary antibodies (1:1000 in TBST with 5% bovine serum albumin) from a commercial vendor (Cell Signaling Technology; Danvers, MA, USA). These antibodies targeted phosphorylated (p-) LATS1 (Thr1079) (cat. no. 8654), p-YAP (Ser127) (cat. no. 4911), p-TAZ (Ser89) (cat. no. 4911), p-mTOR (Ser2448) (cat. no. 5536), p-p70S6K (Thr389)

(cat. no. 9234), and p-rpS6 (Ser235/236) (cat. no. 4858). The following day, membranes were washed for 15 minutes in TBST and incubated with a horseradish peroxidase-conjugated anti-rabbit secondary antibodies diluted 1:2000 in TBST with 5% BSA (cat. no. 7074; Cell Signaling Technology) at room temperature for 1 hour. Membrane development was performed using an enhanced chemiluminescent reagent (cat. no. ELLUF0100, Millipore Sigma; Burlington, MA, USA), and band densitometry was performed using a gel documentation system and associated densitometry software (ChemiDoc Touch, Bio-Rad). Band densities for phosphorylated targets were normalized to corresponding Ponceau densities as we have previously performed with acute bout settings [89], and fold-change values were derived relative to the aggregate PRE mean of the FULL condition.

Experiment 2

Chronic Experimental Design. Experiment 2 employed a within-subject contralateral limb design over 8 weeks using the 45-degree leg press, seated knee extension, and lying knee flexion exercises. One leg was assigned to FULL and the contralateral leg to LP for the duration of the intervention, and again participants were block randomized by limb to counterbalance for limb dominance. Participants first completed an informed consent and phenotyping visit including health history screening, body composition assessment using bioelectrical impedance spectroscopy (SFB7, Impedimed; Carlsbad, CA, USA) and familiarization with the range of motion for each condition on the leg press. Three to five days thereafter, participants attended the Auburn University MRI Research Center in a greater than 4-hour fasted state for pre-intervention lower-body MRI scanning. Participants were instructed to cease resistance training 72

hours prior to the initial MRI scan. One to two days following the MRI scan, pre-intervention bilateral VL biopsies were collected. Participants then completed 16 supervised resistance training sessions across 8 weeks (2 days/week). Eighty-seven to 96 hours after the final training session, participants returned for post-intervention MRI scanning, followed 1 to 2 days later by post-intervention bilateral VL biopsies. Participants were instructed to avoid lower-body resistance training outside of supervised sessions for the duration of the intervention.

Resistance Training Protocol. Exercises were performed in the following order: unilateral leg press (Arsenal Strength Reloaded Linear Leg Press; Arsenal Strength, Lenoir City, TN), unilateral leg extension, and lying leg curl (Life Fitness Signature Series; Life Fitness, Franklin Park, IL). A slant board (20 Degree Slant Board; SquatWedgiez) was adhered to the footplate of the leg press using hook-and-loop tape (Melsan 4x6 Inch Hook and Loop Tape Heavy Duty; Melsan) to allow full knee flexion to be achieved without heel elevation. The seatback of the leg press was positioned one setting from fully reclined for all participants. For the leg press, both conditions performed the exercise to maximal knee flexion, with each participant able to touch their calf to their hamstring at the bottom of each repetition. FULL condition participants completed approximately double the ROM of the LP condition but did not fully lock out the knee at the top of the movement to prevent offloading. LP participants extended to approximately the midpoint of the full ROM. During the LP condition, a metal device was held by a staff member with extensive resistance training supervision experience at the targeted position to provide an audible cue when participants pressed the metal sled plate to the assigned LP extension endpoint. Unilateral

leg extension was performed through either FULL (100–0° knee flexion) or LP (100–50° knee flexion) ranges of motion, monitored visually by certified trainers. Lying leg curl was performed through full individualized ROM for FULL and 0–80° knee flexion for LP to account for greater gastrocnemius involvement in the early portion of the range of motion; the LP endpoint was enforced via a physical block held by a trained researcher. Each repetition was initiated at a controlled tempo and transitioned to maximal intended velocity as fatigue accumulated naturally within the set; this approach was employed to avoid tempo-related biases favoring the lengthened position. Leg press was performed to volitional failure, defined as the point at which the participant believed the next repetition could not be completed or would require compromised form. Leg extension and leg curl were performed to concentric failure, defined as the inability to complete the assigned range of motion. Sets and rest periods were exercise-specific: leg press progressed from 3 sets (sessions 1–9) to 4 sets (sessions 10 onward) with 1.5 minutes of rest between sets, alternating the starting leg each set; leg extension progressed from 3 sets (sessions 1–3) to 4 sets (sessions 4 onward) with 1 minute of rest between sets; and leg curl progressed from 5 sets (sessions 1–5) to 6 sets (sessions 6 onward) with 1 minute of rest between sets. Approximately 2 minutes separated the leg press and leg extension blocks, while the transition from leg extension to leg curl was self-paced.

Leg press kinematics. ROM adherence was confirmed during session 10 of 16, in which participants were fitted with inertial measurement units (IMUs; Noraxon Ultium Motion, Noraxon U.S.A., Scottsdale, AZ) on each shin and thigh to verify that each leg was trained within its assigned range of motion via wireless transmission to myoRESEARCH

software (Noraxon U.S.A., Scottsdale, AZ). Raw joint angle data exported from myoRESEARCH were processed in R (version 4.4.1; R Core Team, 2024). Knee and hip flexion signals were each smoothed using a 7-point centered moving average filter prior to repetition detection. Individual repetitions were identified from peaks in the smoothed knee signal using a minimum peak separation of 0.20 seconds. The first and last repetitions of each set were excluded when four or more repetitions were detected to minimize the influence of transition periods. All processed files were visually inspected to confirm accurate repetition detection. Peak flexion, minimum flexion, and ROM were extracted from each retained repetition and averaged across repetitions within each set, then across sets within each leg.

Magnetic Resonance Imaging. MRI scanning was performed on a 3T SkyraFit system (Siemens, Erlangen, Germany) at the Auburn University MRI Research Center. Participants were positioned prone on the patient table with an approximately 5-minute latency period before scanning. A T1-weighted turbo spin echo pulse sequence was used (repetition time: 1,400 ms; echo time: 23 ms; in-plane resolution: 0.9 × 0.9 mm^2) to obtain transverse image sets spanning the top of the ilium to the patella with a 2-mm slice thickness and no inter-slice gap. All image analysis was performed blinded to training conditions by the same investigator (R.J.B.). DICOM files were preprocessed in OsiriX MD (Pixmeo, Geneva, Switzerland) and imported into 3D Slicer (Brigham and Women's Hospital, Boston, MA), where the polygon tool was used to manually trace VL borders on each image. Image standardization was as follows: i) the most proximal slice was defined as the first axial image in which the gluteal musculature was no longer visible; ii) the most distal slice was

defined as 10 slices (2 cm) proximal to the final image in which the RF was no longer visible; iii) five equidistant slices were selected between the proximal and distal boundaries at both PRE and POST. Total VL mCSA was computed as the sum of mCSA values across the five slices.

Muscle Biopsies. Mid-thigh VL biopsies were obtained using a 5-gauge needle with suction under aseptic conditions as previously described by our laboratory [90]. Approximately 80–140 mg of muscle tissue was excised per biopsy. Tissue allocated for histological analysis was mounted in optimal cutting temperature (OCT) compound, frozen in liquid nitrogen-cooled isopentane, and stored at −80°C. Tissue for molecular analyses was rapidly cleaned of blood, fat, and connective tissue, placed in cryogenic vials, flash frozen in liquid nitrogen, and stored at −80°C.

Immunohistochemistry. Cryosections (12 µm) were cut using a cryostat (Leica Biosystems, Buffalo Grove, IL), adhered to positively charged histological slides, and stored at −80°C until batch processing. All samples from the same participant were processed on the same slide simultaneously. Sections were air-dried for 2 hours at room temperature and fixed in −20°C acetone for 5 minutes. Slides were then incubated with 3% H_2O_2 for 10 minutes, treated with autofluorescence quenching reagent (cat. no. 23007; Biotium, Fremont, CA, USA) for 1 minute and blocked for 1 hour with a solution of 5% goat serum, 2.5% horse serum, and 0.1% Triton-X at room temperature. Thereafter, slides were blocked with a streptavidin and biotin blocking solutions (cat. no. SP-2002; Vector Laboratories; Newark, CA, USA) at room temperature for 15 minutes each, with 5-minute

PBS washes occurring between these incubations. Slides were then incubated overnight at 4°C with primary antibody cocktail containing 1:100 rabbit anti-dystrophin IgG (cat. no. GTX57970; Abcam; Waltham, MA, USA), 1:100 mouse anti-MyHCI IgG2b (clone: BA-D5; Developmental Studies Hybridoma Bank; Iowa City, IA, USA), and 1:20 mouse anti-PAX7 IgG1 (Developmental Studies Hybridoma Bank) + 2.5% horse serum in PBS. The following day, slides were washed four times (5 minutes each) in PBS and incubated for 90 minutes in biotin-SP-conjugated goat anti-mouse IgG1 (1:1,000) (cat. no. 111-065-003; Jackson ImmunoResearch; West Grove, PA, USA) in 2.5% BSA for 90 minutes. This step was followed by three 5-minute PBS washes and a 60-minute incubation with a solution containing 1:500 streptavidin (cat. no. S911; Thermo Fisher Scientific), 1:250 goat anti-mouse IgG2b Alexa Fluor 488 (cat. no. A21141; Thermo Fisher Scientific) and 1:250 goat anti-rabbit IgG Alexa Fluor 647 (cat. no. A21245; Thermo Fisher Scientific) in PBS. Following three 5-minute PBS washes, slides underwent a 20-minute incubation with 1:200 Alexa Fluor 555 tyramide (cat. no. B40955; Thermo Fisher Scientific) in PBS. Following three 5-minute PBS washes nuclei were stained with DAPI (1:10,000; cat. no. D3571; Thermo Fisher Scientific) for 10 minutes, washed twice (5 minutes each) in PBS, and sections were mounted with 1:1 PBS/glycerol. Digital images were acquired at 10× (fCSA) and 20× (nuclei as well as satellite cells) objectives using a fluorescent microscope (Zeiss Axio Imager.M2 with motorized stage). Image analysis was automated using MyoVision v1.0 [91] for fiber type-specific fCSA and myonuclei per fiber. Satellite cells were manually counted by an investigator blinded to training conditions (C.A.E.) and expressed as number per 100 fibers (DAPI-positive & PAX7-positive cells within the dystrophin border).

Total RNA Content. Approximately 20 mg of muscle tissue was homogenized in Trizol (cat. no. 15596026; ThermoFisher) per manufacturer's instructions. RNA pellets were reconstituted in 30 µL of diethyl pyrocarbonate (DEPC)-treated water and quantified in duplicate using a NanoDrop Lite spectrophotometer (ThermoFisher). Total RNA content was normalized to input tissue wet weight and expressed as ng RNA per mg tissue, a validated surrogate of muscle ribosome content [50].

Statistical Analysis

All statistical analyses were conducted in R using the lme4 and lmerTest packages. For Experiment 1 western blot outcomes and all Experiment 2 outcomes, a linear mixed-effects model (LMM) was fitted with Condition (FULL vs. LP), Time (PRE vs. POST for Experiment 2; PRE vs. 0h/3h/24h POST for Experiment 1), and their Condition × Time interaction as fixed effects. To account for the contralateral-limb design and repeated measurements, random intercepts were included for participant and for participant-by-condition, reflecting that each participant contributed both a FULL and LP limb measured at multiple points. Estimated marginal means, standard errors, 95% confidence intervals, and planned contrasts were derived using the emmeans package. For Experiment 1 western blot outcomes, follow-up pairwise comparisons between conditions at each timepoint were conducted with Sidak adjustment when a significant Condition × Time interaction was observed. For significant main effects of Time in the absence of a significant Condition × Time interaction, contrasts versus PRE collapsed across conditions were conducted with Sidak adjustment. Statistical significance was set at $\alpha = 0.05$. However, interpretation focused on the magnitude and precision of estimated effects

rather than statistical significance alone. Because equivalence margins were not prespecified, non-significant Condition × Time interactions were interpreted as indicating no clear evidence of a differential response between conditions, rather than formal statistical equivalence. To confirm the ROM manipulation, paired t-tests were used to compare FULL and LP conditions for knee and hip ROM and peak flexion angles at session 10, with each participant contributing one value per condition averaged across sets. Data are presented as estimated marginal means ± SE unless otherwise noted; descriptive characteristics are presented as mean ± SD. For Experiment 1 transcriptomic analyses, the statistical approach is described in the Transcriptomics section above.

Results

Participant Characteristics

Experiment 1 included 8 resistance-trained men (22 ± 1 years old, training experience: 5.6 ± 1 years) with a body mass of 92.4 ± 17.1 kg, DXA percent fat of 15.7 ± 5.6, and fat-free mass index of 21.0 ± 2.3 kg lean mass/m^2. Experiment 2 enrolled 18 participants, of whom 2 withdrew (one before the intervention commenced for reasons unrelated to the study, and one due to knee pain), leaving 16 participants who completed the study. Hence, the 16 finishers in Experiment 2 were 26 ± 5 years old (training experience: 8.0 ± 4.9 years) with a body mass of 86.3 ± 9.4 kg, BIS percent fat of 18.2 ± 4.4, and fat-free mass index of 21.5 ± 1.2 kg lean mass/m^2. For Experiment 2 biopsy outcomes, two participants were excluded from individual histological analyses given that tissue yield

or quality was insufficient. Final sample sizes for fCSA, myonuclei, and SC analyses are reported in the results.

Experiment 1: Acute Anabolic Phospho- Signaling

Hippo and mTORC1 signaling protein data are presented in Figure 2. Phosphorylated LATS1 (Thr1079) demonstrated a significant Condition × Time interaction ($P = 0.010$), with post hoc analysis revealing FULL was greater than LP at 24h post ($P = 0.004$) (Fig. 2a). Phosphorylated YAP (Ser127) demonstrated a significant main effect of Time ($P = 0.037$), with values at 3h post lower than PRE ($P = 0.015$), but no Condition × Time interaction ($P = 0.550$) (Fig. 2b). Phosphorylated TAZ (Ser89) showed no significant main effect of Time ($P = 0.249$) and no Condition × Time interaction ($P = 0.244$) (Fig. 2c). For mTORC1 targets, phosphorylated mTOR (Ser2448) showed a significant main effect of Time ($P = 0.010$), with values at 0h post greater than PRE ($P = 0.023$), and no Condition × Time interaction ($P = 0.787$) (Fig. 2d). Phosphorylated p70S6K (Thr389) showed no significant main effect of Time ($P = 0.231$) and no Condition × Time interaction ($P = 0.166$) (Fig. 2e). Phosphorylated rpS6 (Ser235/236) demonstrated a significant main effect of Time ($P = 0.033$), with values at 0h post greater than PRE ($P = 0.038$), and no Condition × Time interaction ($P = 0.353$) (Fig. 2f). A representative Western blot for all targets is presented in Fig. 2g.

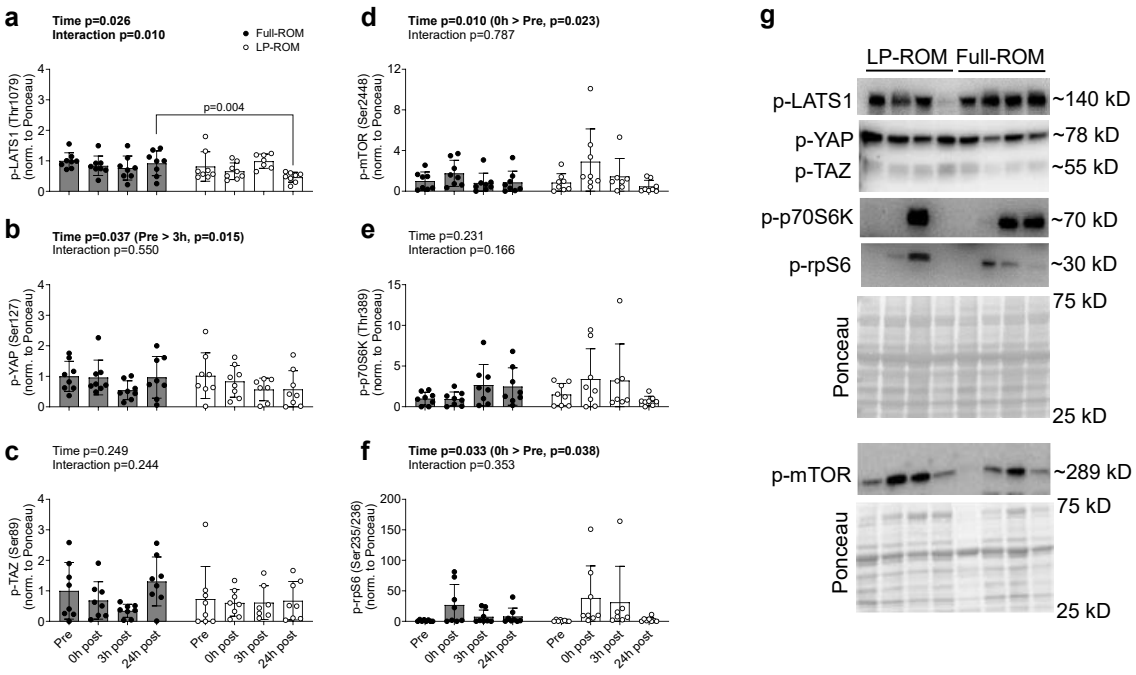

FIGURE 2. Experiment 1 Hippo and mTORC1 signaling protein data. Panels depict phosphorylated protein expression (normalized to Ponceau) for (a) p-LATS1 (Thr1079), (b) p-YAP (Ser127), (c) p-TAZ (Ser89), (d) p-mTOR (Ser2448), (e) p-p70S6K (Thr389), and (f) p-rpS6 (Ser235/236) in the VL of n=8 participants at PRE, 0h, 3h, and 24h post-exercise following Full-ROM (filled circles) and LP-ROM (open circles) leg extension bouts. Representative western blot images and Ponceau stain are also presented. Time and Condition × Time interaction P values from LMMs are shown above each panel; bolded interaction P values indicate $P < 0.05$. Bars represent means ± standard deviation values with individual participant values are shown as dots.

Experiment 1: Acute Transcriptomic Responses

Both LP and FULL conditions produced progressive increases in the number of differentially expressed mRNAs relative to PRE across the post-exercise time course. Upregulated mRNAs relative to PRE were 31 (FULL) and 18 (LP) at 0h, 707 and 469 at 3h, and 1,344 and 1,242 at 24h post-exercise (Fig. 3a). Downregulated mRNAs were 9 (FULL) and 8 (LP) at 0h, 157 and 76 at 3h, and 1,379 and 975 at 24h post-exercise (Fig. 3b). mRNAs showing significant interactions were 22 (up in FULL) and 9 (up in LP) from Pre to 0h, 20 (up

in FULL) and 24 (up in LP) from Pre to 3h, and were 35 (up in FULL) and 5 (up in LP) from Pre to 24h post-exercise (Fig. 3c). Enriched Gene Ontology (GO) pathways from upregulated mRNAs within-condition were absent from Pre to 0h in both conditions, with 34 (up in FULL) and 15 (up in LP) enriched pathways from Pre to 3h, and 38 (up in FULL) and 50 (up in LP) Pre to 24h post-exercise (Fig. 3d). Minimal GO pathway enrichment was observed from downregulated mRNAs (Fig. 3e). Moreover, no enriched pathways were evident from the limited number of mRNAs (seen in Fig. 3c) exhibiting significant interactions (Fig. 3f).

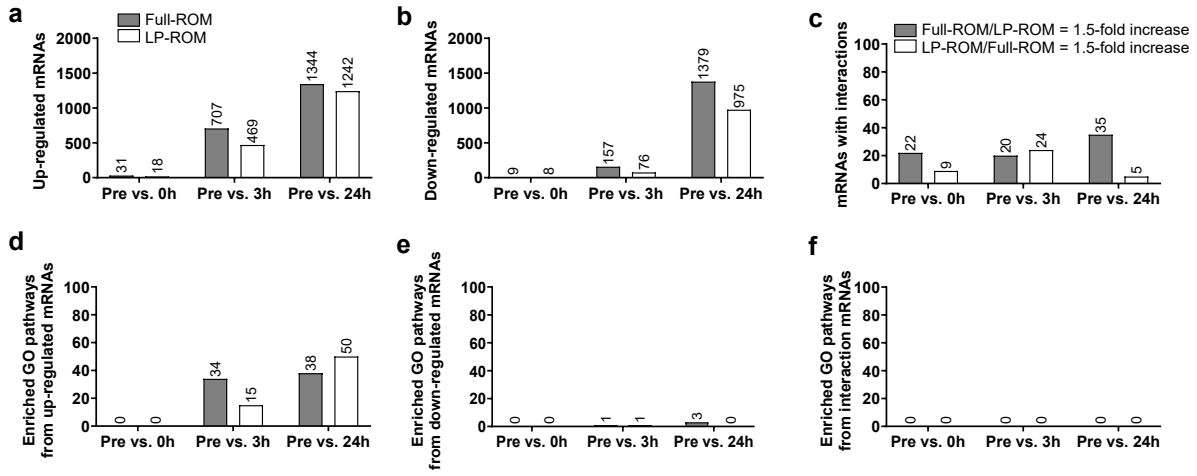

FIGURE 3. Experiment 1 summary of transcriptomic data. Full-ROM (gray bars) and LP-ROM (open bars) leg extension bouts in the VL of n=8 resistance-trained men. Panels depict (a) the number of up-regulated mRNAs within each condition relative to Pre, (b) down-regulated mRNAs within each condition relative to Pre, (c) mRNAs exhibiting between-condition interactions, (d) enriched Gene Ontology (GO)-Slim biological pathways from up-regulated mRNAs within each condition, (e) enriched GO-Slim pathways from down-regulated mRNAs within each condition, and (f) enriched GO-Slim pathways from mRNAs demonstrating interactions.

Figure 4 provides additional context related to the within-leg protocol transcriptomic changes from Pre to 3h post-exercise (Fig. 4a&b) as well as Pre to 24h post-exercise (Fig.

4c&d). Two conserved GO-Slim biological pathways were evident within protocols based on upregulated mRNAs from Pre to 3h post-exercise and included “inflammatory response” (GO:0006954) and “regulation of angiogenesis” (GO:0045765). Moreover, 13 of the top 20 up-regulated mRNAs within protocols from Pre to 3h post-exercise (based on fold-change) were conserved. Several conserved GO-Slim biological pathways were evident within protocols based on upregulated mRNAs from Pre to 24h post-exercise, and 14 of the top 20 up-regulated mRNAs within protocols from Pre to 3h post-exercise were also conserved.

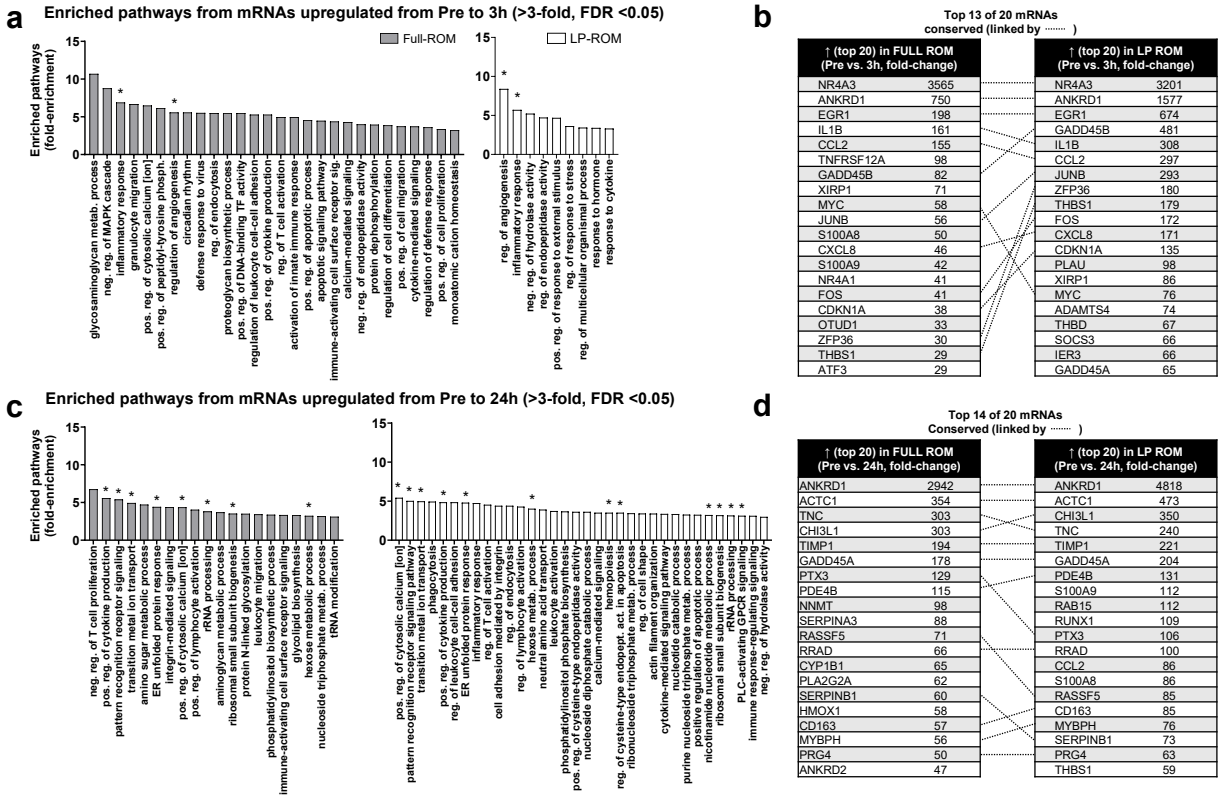

FIGURE 4. Experiment 1 details of enriched GO-Slim biological pathways and top up-regulated mRNAs within each condition. Full-ROM (gray bars) and LP-ROM (open bars) leg extension bouts in the VL of n=8 resistance-trained men. Panels depict (a) the top GO-Slim biological pathways predicted to be enriched based on up-regulated mRNAs in both protocols from Pre to 3h post-exercise, (b) the top 20 up-regulated mRNAs in both

protocols from Pre to 3h post-exercise, (c) the top GO-Slim biological pathways predicted to be enriched based on up-regulated mRNAs in both protocols from Pre to 24h post-exercise, (d) up-regulated mRNAs in both protocols from Pre to 24h post-exercise. Note: * in panels a & c depict conserved pathways between protocols at the Pre to 3h or Pre to 24h comparisons, and dashed lines in panels b&d (---------) depict conserved mRNAs between protocols.

Experiment 2: Kinematics

Peak and minimum joint angles during the leg press exercise, measured at session 10, are presented in Figure 5, with individual participant data shown for each condition. For the hip, peak flexion was similar between conditions (FULL: 103.9 ± 13.2°; LP: 106.8 ± 9.2°; P = 0.094), while minimum hip flexion differed markedly (FULL: 62.1 ± 12.1°; LP: 85.8 ± 9.8°), resulting in a substantially greater hip ROM in FULL compared to LP (41.8 ± 7.7° vs. 21.0 ± 3.4°; t(14) = 10.45, P < 0.001). For the knee, peak flexion was again similar between conditions (FULL: 123.7 ± 11.7°; LP: 126.2 ± 12.6°; P = 0.328), while minimum knee flexion differed markedly (FULL: 31.0 ± 10.4°; LP: 78.3 ± 10.8°), resulting in a substantially greater knee ROM in FULL compared to LP (92.7 ± 10.5° vs. 47.9 ± 8.7°; t(14) = 15.44, P < 0.001). Collectively, these data confirm that the LP condition achieved approximately half the ROM of FULL at both the knee and hip, consistent with the intended manipulation.

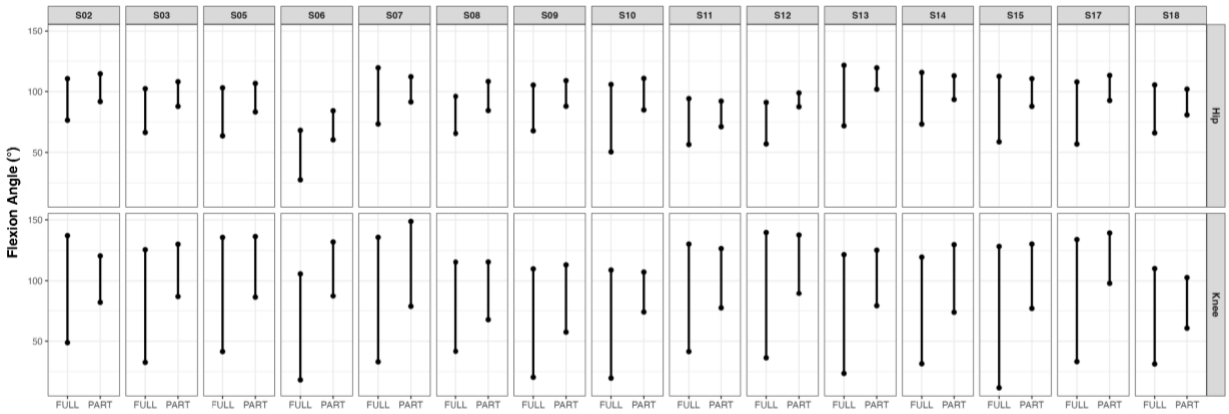

FIGURE 5. Knee and hip flexion angle ranges during the leg press exercise recorded at session 10 from the lower body of n=15 trained men. Each panel displays individual participant data for Full-ROM (FULL) and lengthened partial-ROM (LP) conditions. Filled circles represent peak (upper) and minimum (lower) flexion angles averaged across sets within the session.

Experiment 2: VL Muscle Cross-Sectional Area

VL mCSA data are presented in Figure 6. Total VL mCSA, summed across five equidistant MRI-derived transverse slices increased from PRE to POST when conditions were collapsed, indicating evidence of VL hypertrophy over the intervention period (main effect of Time estimate: 9.3 cm^2, [6.8, 11.8], $P < 0.001$), FULL increased from 166.0 ± 6.7 to 175.9 ± 6.7 cm^2, and LP increased from 164.7 ± 6.7 to 173.4 ± 6.7 cm^2. There was no clear evidence of a differential change between conditions (Condition × Time contrast estimate: -1.4 cm^2, 95% CI [−6.1, 3.4], $P = 0.640$).

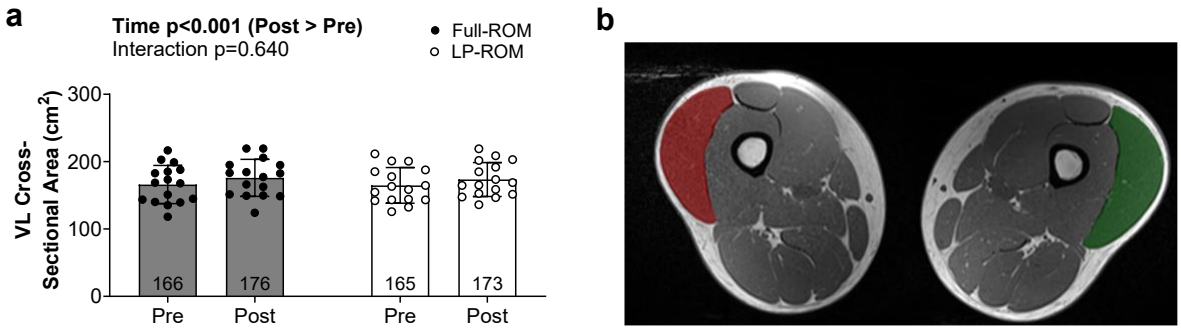

FIGURE 6. Experiment 2 VL muscle cross-sectional area data. Results are from n=16 participants. Panels depict (a) total VL mCSA summed across five equidistant MRI-derived transverse slices at PRE and POST for Full-ROM (filled circles) and LP-ROM (open circles) training conditions. Bars represent means ± standard deviation values with individual participant values are shown as dots. Time and Condition × Time interaction P values from LMMs are shown above. (b) Representative transverse MRI images showing VL segmentation (red = FULL leg PRE; green = LP leg POST) at mid-thigh from the same participant.

Experiment 2: Fiber Type-Specific Cross-Sectional Area

Type I fCSA and myonuclei per fiber data are presented in Fig. 7a&c. Type I fCSA did not provide clear evidence of an overall PRE-to-POST change when conditions were collapsed (main effect of Time estimate: 241 μm^2, 95% CI [−242, 724], $P = 0.314$). Estimated marginal means were 5,123 ± 318 μm^2 at PRE and 5,194 ± 318 μm^2 at POST in FULL, and 5,280 ± 318 μm^2 at PRE and 5,703 ± 327 μm^2 at POST in LP. There was no clear evidence of a differential change between conditions (Condition × Time contrast estimate: 339 μm^2, 95% CI [−627, 1305], $P = 0.476$). Similarly, Type I myonuclei per fiber did not provide clear evidence of an overall PRE-to-POST change when conditions were collapsed (main effect of Time estimate: −0.22, 95% CI [−0.60, 0.16], $P = 0.245$). Estimated marginal means were 2.39 ± 0.19 at PRE and 2.13 ± 0.19 at POST in FULL, and 2.35 ± 0.20 at PRE and 2.18 ± 0.20 at POST in LP. There was no clear evidence of a differential change between conditions (Condition × Time contrast estimate: 0.09, 95% CI [−0.67, 0.85], $P = 0.813$).

Type II fCSA and myonuclei per fiber data are presented in Fig. 7b&d. Type II fCSA did not provide clear evidence of an overall PRE-to-POST change when conditions were collapsed (main effect of Time estimate: 14.5 μm^2, 95% CI [−569, 599], $P = 0.956$). Estimated marginal means were 6,630 ± 402 μm^2 at PRE and 6,374 ± 402 μm^2 at POST in FULL, and 6,628 ± 401 μm^2 at PRE and 6,913 ± 413 μm^2 at POST in LP. There was no clear evidence of a differential change between conditions (Condition × Time contrast estimate: 541 μm^2, 95% CI [−627, 1709], $P = 0.350$). Similarly, Type II myonuclei per fiber did not provide clear evidence of an overall PRE-to-POST change when conditions were collapsed (main effect of Time estimate: −0.09, 95% CI [−0.49, 0.31], $P = 0.653$). Estimated marginal

means were 3.09 ± 0.25 at PRE and 2.89 ± 0.25 at POST in FULL, and 3.02 ± 0.26 at PRE and 3.03 ± 0.26 at POST in LP. There was no clear evidence of a differential change between conditions (Condition × Time contrast estimate: 0.21, 95% CI [−0.59, 1.01], $P = 0.589$).

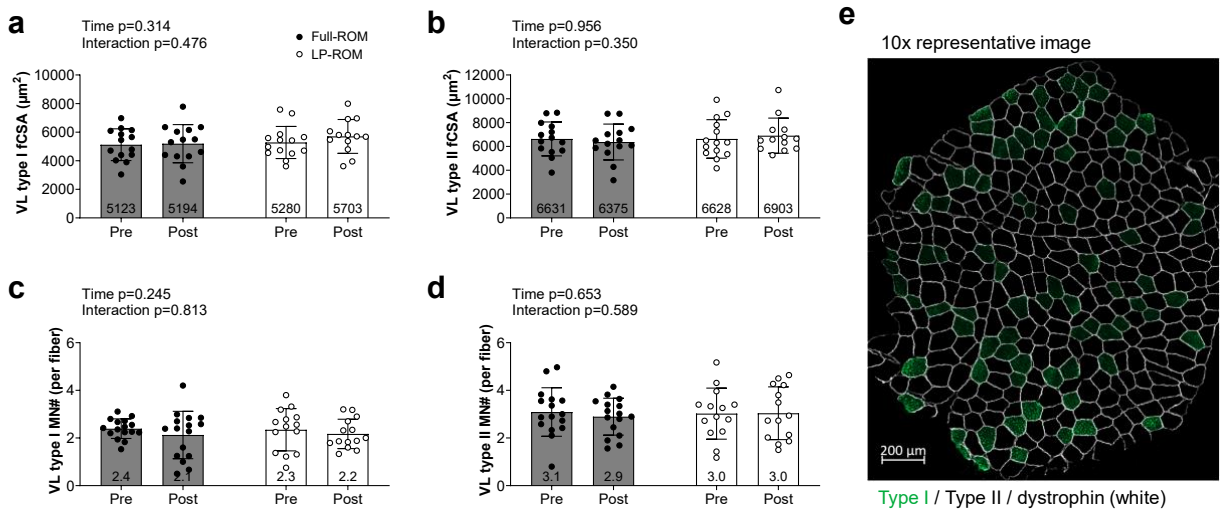

FIGURE 7. Experiment 2 VL fiber cross-sectional area and myonuclei data. Panels depict (a) Type I fCSA, (b) type II fCSA, (c) type I myonuclei per fiber, and (d) type II myonuclei per fiber at PRE and POST for Full-ROM (filled circles) and LP-ROM (open circles) conditions. Data are from 14 of the 16 participants due to two participants not yielding tissue quantity or quality sufficient for analyses. Bars represent means ± standard deviation values with individual participant values are shown as dots. Time and Condition × Time interaction P values are shown above each panel. (e) Representative 10× fluorescence microscopy image from one participant showing type I fibers (Alexa Fluor 488), type II fibers (not stained), and dystrophin (Alexa Fluor 647, pseudo-colored white border).

Experiment 2: Satellite Cell Number, and Total RNA Content

Satellite cell and total RNA data are presented in Figure 8. Type I satellite cell number did not provide clear evidence of an overall PRE-to-POST change when conditions were collapsed (main effect of Time estimate: 1.9, 95% CI [−1.0, 4.7], $P = 0.186$). Estimated marginal means were 9.1 ± 3.0 at PRE and 8.7 ± 3.0 at POST in FULL, and 8.8 ± 3.0 at PRE

and 13.1 ± 3.1 at POST in LP. There was no clear evidence of a differential change between conditions (Condition × Time contrast estimate: 4.7, 95% CI [−1.0, 10.3], *P* = 0.102). In contrast, Type II satellite cell number increased from PRE to POST when conditions were collapsed, indicating evidence of satellite cell accretion over the intervention period (main effect of Time estimate: 8.3, 95% CI [2.2, 14.4], *P* = 0.001); however, there was no clear evidence of a differential change between conditions (Condition × Time contrast estimate: 1.6, 95% CI [−10.7, 13.8], *P* = 0.797), and estimated marginal means were 11.5 ± 3.9 at PRE and 19.0 ± 3.9 at POST in FULL, and 7.8 ± 3.9 at PRE and 16.9 ± 4.0 at POST in LP.

Total RNA content did not provide clear evidence of an overall PRE-to-POST change when conditions were collapsed (main effect of Time estimate: 23.5 ng/mg, 95% CI [−45.9, 93.0], *P* = 0.495). Estimated marginal means were 394 ± 34 ng/mg at PRE and 396 ± 34 ng/mg at POST in FULL, and 421 ± 34 ng/mg at PRE and 465 ± 34 ng/mg at POST in LP. There was no clear evidence of a differential change between conditions (Condition × Time contrast estimate: 42.5 ng/mg, 95% CI [−96.4, 181.0], *P* = 0.537).

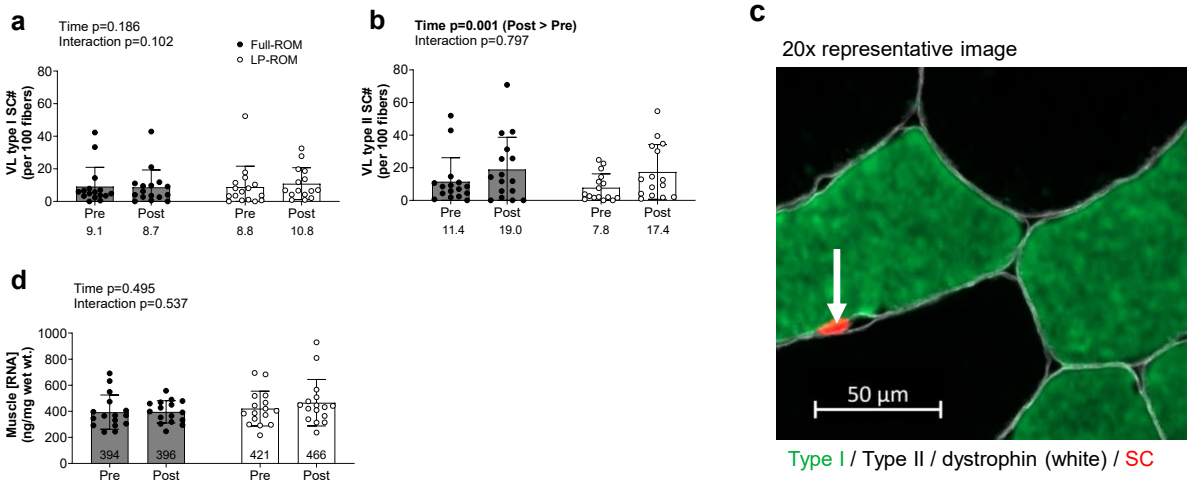

FIGURE 8. Experiment 2 VL satellite cell number and total RNA content. Panels depict (a) Type I SC per 100 fibers and (b) type II SC per 100 fibers at PRE and POST for Full-ROM (filled circles) and LP-ROM (open circles) conditions. Data are from 14 participants for satellite cells and 16 for total RNA. (c) Representative 20× fluorescence microscopy image from one participant showing type I/type II fibers, dystrophin (pseudocolored white border), and a type I fiber satellite cell (within the dystrophin border). (d) Total RNA content (ng/mg wet tissue) at PRE and POST. Bars represent means ± standard deviation values with individual participant values are shown as dots. Time and Condition × Time interaction P values are shown above each panel.

Discussion

The primary finding of this investigation is that 8 weeks of LP and FULL lower-body resistance training produced increases in VL size, with no clear evidence that hypertrophic or cellular responses differed between conditions in resistance-trained men. Summed VL mCSA values across five MRI-derived equidistant images increased significantly with training in both conditions, confirming that both protocols elicited hypertrophy. However, Condition × Time contrasts did not provide clear evidence of differential change between LP and FULL for any outcome, including VL mCSA, fiber type-specific CSA, myonuclei per fiber, satellite cell number, or total RNA content. In the accompanying acute study, both conditions produced broadly similar time-dependent transcriptomic changes and anabolic signaling responses. The following paragraphs expand upon these null findings.

In experiment 1, both LP and FULL protocols produced remarkably conserved acute transcriptional and signaling responses in the VL. This was evident through similar enriched GO-Slim biological pathways from upregulated mRNAs shared across conditions at 3h and 24h post-exercise (as well as conserved top-upregulated mRNAs themselves). Regardless of protocol, these pathway-level findings are broadly consistent with the

resistance exercise transcriptomics literature. The MetaMEx meta-analysis conducted by Pillon and colleagues integrating data from 66 skeletal muscle transcriptomic datasets, including 8 studies of acute resistance exercise, identified the inflammatory and angiogenesis responses as one of the most consistently enriched GO terms among upregulated genes in the 2–4h window following acute resistance exercise in healthy humans [92]. A subsequent analysis from the same group employing the MetaMEx database to construct a transcriptional timeline from 0 to 48h after acute exercise revealed that inflammatory response and cytokine signaling pathways are characteristically induced in skeletal muscle [93], mirroring the 24h timepoint at which these pathways emerged in the present study. Importantly, the presence of the inflammatory response in these resistance-trained participants should not be interpreted solely as a marker of exercise-induced muscle damage. Rather, the transcriptional upregulation of inflammatory mediators likely reflects regulated remodeling that facilitates satellite cell recruitment, extracellular matrix turnover, and protein turnover, and these responses even persist in experienced trainees as sampled in the current study [92]. The Hippo and mTORC1 signaling data also largely showed no acute between-condition differences over time. The one significant Condition × Time interaction observed was for phosphorylated LATS1 (Thr1079), a component of the Hippo signaling pathway, which was higher in FULL relative to LP at the 24-hour post-exercise timepoint ($P = 0.004$). The Hippo pathway has been implicated in mechanosensory transduction and load-dependent gene regulation and LATS1 phosphorylation at Thr1079 reflects kinase activation that generally suppresses downstream YAP/TAZ activity [94]. However, the biological significance of this

isolated interaction is difficult to interpret in the absence of corresponding differences in transcriptomic or Experiment 2 hypertrophic outcomes. Hence, the high overlap in mRNA and phospho-signaling responses suggests both conditions impose a qualitatively comparable mechanical challenge on the VL muscle.

In Experiment 2, the absence of significant training effects on fiber type-specific fCSA in either condition also warrants consideration. Overall VL mCSA increased significantly, albeit modestly, confirming that whole-muscle hypertrophy occurred. The MRI finding is likely related to resistance training in previously trained individuals producing smaller relative increases in skeletal muscle hypertrophy compared to untrained populations [95]. Further, 8 weeks at two sessions per week may be insufficient to detect significant fiber-level hypertrophy due to the small tissue sampling with biopsy analysis along with variation in this measure as our laboratory and others have previously posited in prior reviews and original investigations [96-98]. It is also worth noting that the lack of biopsy-derived fCSA increases in the context of VL hypertrophy likely reflects a localized sample at a fixed mid-thigh site that may not capture the regional distribution of hypertrophy across the muscle as comprehensively as MRI. The multi-site VL MRI data, therefore, provide a more sensitive and anatomically complete estimate of hypertrophic response in this study.

Both Experiment 2 conditions also produced a significant increase in type II satellite cell number over the 8-week intervention, with no clear evidence that this response differed between LP and FULL. Satellite cells are essential for long-term muscle fiber remodeling and their expansion with resistance training is well-established in trained

populations [55, 58]. The similar pattern of satellite cell responses observed between LP and FULL further supports the conclusion that ROM does not fundamentally alter the cellular remodeling environment in the VL. Total RNA content, a validated surrogate of muscle ribosome content, did not increase significantly in either condition. This finding is consistent with prior data from our laboratory indicating that shorter-term resistance training programs in individuals with prior training experience does not increase this outcome [99]. Moreover, the substantial inter-individual variability in this measure, evidenced by wide confidence intervals, may also have limited statistical power to detect a training effect. Regardless, the absence of a condition difference in total RNA reinforces that LP and FULL imposed a comparable stimulus with respect to translational machinery remodeling in the VL.

Critically, there is a biomechanical premise which may help explain the null findings across both experiments. For Experiment 2, deep knee flexion during FULL ROM leg press positions the VL is a more lengthened state while substantial external moment demand is present [100], meaning conventional FULL training already imposes considerable mechanical challenge at long VL lengths. Although a full ROM leg extension, as performed on conventional weight stack machines during both experiments, presents a shortened-dominant resistance challenge to the VL, its inclusion within a broader multi-exercise program alongside the leg press in Experiment 2 may have rendered its resistance profile a negligible determinant of the overall hypertrophic stimulus when considered within the context of the full program. The present Experiment 1 and 2 findings are broadly consistent with prior work in the quadriceps suggesting that VL hypertrophy is not strongly influenced

by ROM differences within a practically relevant range. For instance, squat depth studies have generally shown that knee flexion beyond approximately 90° does not further enhance VL hypertrophy compared to shallower depths [6], and the present Experiment 2 data extend this to a direct comparison of LP versus FULL training across multiple lower-body exercises in trained individuals.

Experimental considerations

Several limitations should be acknowledged. Experiment 1 included 8 participants, limiting statistical power for the acute outcomes and precluding strong inferences about individual differences in signaling response. Second, we did not measure sarcomere length, serial sarcomere number, or fascicle length, which would provide additional mechanistic insight into potential architectural adaptations. Third, only younger trained men were examined herein, and these results do not reflect potential adaptations that may be observed in other populations. Finally, the sample was exclusively resistance-trained males, and results may not generalize to other populations.

Conclusions

In conclusion, both the LP and FULL ROM conditions produced increased VL size and similar patterns of cellular adaptation over 8 weeks in resistance-trained men, as assessed by MRI-derived CSA, fiber type-specific CSA, myonuclei per fiber, SC number, and total RNA content. Acute transcriptomic and anabolic signaling responses were likewise comparable between conditions. These findings suggest both ROM strategies are

effective for promoting VL hypertrophy in trained populations. However, chronic outcomes should be interpreted in the context of experiment 2's full lower-body program where the full ROM leg press still challenged the VL at longer lengths regardless of condition, potentially attenuating any length-dependent advantage. Future work should attempt to replicate these findings and further delineate the boundary conditions under which length-dependent hypertrophy is most robustly observed.

ADDITIONAL INFORMATION

Acknowledgments
We graciously thank the participants for partaking in this study.

Research ethics
Experiment 1 was approved by the University of Mary Hardin-Baylor's IRB (IRB protocol no. LT81725). Experiment 2 was approved by the Auburn University IRB (IRB protocol no. STUDY00000282).

Informed consent statement
All participants in Experiments 1 and 2 were provided with ample information about study procedures and provided verbal and written consent prior to engaging in protocols.

Authorship contribution statement
DLP primarily drafted the manuscript with the assistance of MDR. DRT, TG, JK, MR, JQ, CDW, MM-V, VR-C, AB, RJB, CAE, and CGV aided in multiple aspects of data collection and/or analysis warranting co-authorship. LLT supervised and oversaw Experiment 1 execution. This project served as DLP's dissertation works, and project supervision was provided by CBM, RB, ANK, and DTB. All co-authors were provided with the opportunity to edit the work and agree to the manuscript's submission.

Funding
The study was supported by a seed grant from the Edward Via College of Osteopathic Medicine awarded to DLP, DTB, HB, and MDR. DRT is funded through an Auburn University College of Education Dean's Research Fellowship.

Declaration of competing interests
None of the authors have conflicts of interest to declare in relation to the current data.

Data availability

Raw data related to the study outcomes will be provided upon reasonable request by emailing mdr0024@auburn.edu.

References

1. Currier, B.S., et al., *Resistance training prescription for muscle strength and hypertrophy in healthy adults: a systematic review and Bayesian network meta-analysis.* Br J Sports Med, 2023. **57**(18): p. 1211-1220.
2. Maeo, S., et al., *Greater Hamstrings Muscle Hypertrophy but Similar Damage Protection after Training at Long versus Short Muscle Lengths.* Med Sci Sports Exerc, 2021. **53**(4): p. 825-837.
3. Larsen, S., et al., *The effects of hip flexion angle on quadriceps femoris muscle hypertrophy in the leg extension exercise.* J Sports Sci, 2025. **43**(2): p. 210-221.
4. Kinoshita, M., et al., *Triceps surae muscle hypertrophy is greater after standing versus seated calf-raise training.* Front Physiol, 2023. **14**: p. 1272106.
5. Kassiano, W., et al., *Greater Gastrocnemius Muscle Hypertrophy After Partial Range of Motion Training Performed at Long Muscle Lengths.* J Strength Cond Res, 2023. **37**(9): p. 1746-1753.
6. McMahon, G.E., et al., *Impact of range of motion during ecologically valid resistance training protocols on muscle size, subcutaneous fat, and strength.* J Strength Cond Res, 2014. **28**(1): p. 245-55.
7. Pedrosa, G.F., et al., *Training in the Initial Range of Motion Promotes Greater Muscle Adaptations Than at Final in the Arm Curl.* Sports (Basel), 2023. **11**(2).
8. Wolf, M., et al., *Lengthened partial repetitions elicit similar muscular adaptations as full range of motion repetitions during resistance training in trained individuals.* PeerJ, 2025. **13**: p. e18904.
9. Werkhausen, A., et al., *Adaptations to explosive resistance training with partial range of motion are not inferior to full range of motion.* Scand J Med Sci Sports, 2021. **31**(5): p. 1026-1035.
10. Kubo, K., T. Ikebukuro, and H. Yata, *Effects of squat training with different depths on lower limb muscle volumes.* Eur J Appl Physiol, 2019. **119**(9): p. 1933-1942.
11. Pinto, R.S., et al., *Effect of range of motion on muscle strength and thickness.* J Strength Cond Res, 2012. **26**(8): p. 2140-5.
12. Roberts, M.D., et al., *Mechanisms of mechanical overload-induced skeletal muscle hypertrophy: current understanding and future directions.* Physiol Rev, 2023. **103**(4): p. 2679-2757.
13. Rosenfeldt, M., et al., *Comparison of resistance training vs static stretching on flexibility and maximal strength in healthy physically active adults, a randomized controlled trial.* BMC Sports Sci Med Rehabil, 2024. **16**(1): p. 142.
14. Massini, D.A., et al., *The Effect of Resistance Training on Bone Mineral Density in Older Adults: A Systematic Review and Meta-Analysis.* Healthcare (Basel), 2022. **10**(6).
15. Prevett, C., et al., *Role of Resistance Training in Mitigating Risk for Mobility Disability in Community-Dwelling Older Adults: A Systematic Review and Meta-analysis.* Arch Phys Med Rehabil, 2022. **103**(10): p. 2023-2035.
16. Landrigan, J.F., et al., *Lifting cognition: a meta-analysis of effects of resistance exercise on cognition.* Psychol Res, 2020. **84**(5): p. 1167-1183.

17. Lee, S., et al., *Effects of aerobic versus resistance exercise without caloric restriction on abdominal fat, intrahepatic lipid, and insulin sensitivity in obese adolescent boys: a randomized, controlled trial*. Diabetes, 2012. **61**(11): p. 2787-95.
18. Stamatakis, E., et al., *Does Strength-Promoting Exercise Confer Unique Health Benefits? A Pooled Analysis of Data on 11 Population Cohorts With All-Cause, Cancer, and Cardiovascular Mortality Endpoints*. Am J Epidemiol, 2018. **187**(5): p. 1102-1112.
19. Kim, G. and J.H. Kim, *Impact of Skeletal Muscle Mass on Metabolic Health*. Endocrinol Metab (Seoul), 2020. **35**(1): p. 1-6.
20. Wolfe, R.R., *The underappreciated role of muscle in health and disease*. Am J Clin Nutr, 2006. **84**(3): p. 475-82.
21. Huxley, H. and J. Hanson, *Changes in the cross-striations of muscle during contraction and stretch and their structural interpretation*. Nature, 1954. **173**(4412): p. 973-6.
22. Williams, C.D., et al., *The length-tension curve in muscle depends on lattice spacing*. Proc Biol Sci, 2013. **280**(1766): p. 20130697.
23. Granzier, H.L., H.A. Akster, and H.E. Ter Keurs, *Effect of thin filament length on the force-sarcomere length relation of skeletal muscle*. Am J Physiol, 1991. **260**(5 Pt 1): p. C1060-70.
24. Huxley, H.E., *Electron Microscope Studies on the Structure of Natural and Synthetic Protein Filaments from Striated Muscle*. J Mol Biol, 1963. **7**: p. 281-308.
25. Walker, S.M. and G.R. Schrodt, *I segment lengths and thin filament periods in skeletal muscle fibers of the Rhesus monkey and the human*. Anat Rec, 1974. **178**(1): p. 63-81.
26. Gokhin, D.S., et al., *Thin-filament length correlates with fiber type in human skeletal muscle*. Am J Physiol Cell Physiol, 2012. **302**(3): p. C555-65.
27. Andrews, M.H., et al., *Multiscale hamstring muscle adaptations following 9 weeks of eccentric training*. J Sport Health Sci, 2025. **14**: p. 100996.
28. Pincheira, P.A., et al., *Biceps femoris long head sarcomere and fascicle length adaptations after 3 weeks of eccentric exercise training*. J Sport Health Sci, 2022. **11**(1): p. 43-49.
29. Wolf, M., et al., *Does longer-muscle length resistance training cause greater longitudinal growth in humans? A systematic review*. Sports Med Health Sci, 2026. **8**(1): p. 34-42.
30. Blazevich, A.J., W. Herzog, and J.P. Nunes, *Triggering sarcomerogenesis: Examining key stimuli and the role attributed to eccentric training-Historical, systematic, and meta-analytic review*. J Sport Health Sci, 2025. **14**: p. 101073.
31. Jorgenson, K.W., et al., *A novel imaging method (FIM-ID) reveals that myofibrillogenesis plays a major role in the mechanically induced growth of skeletal muscle*. Elife, 2024. **12**.
32. Roberts, M.D., et al., *Sarcoplasmic Hypertrophy in Skeletal Muscle: A Scientific "Unicorn" or Resistance Training Adaptation?* Front Physiol, 2020. **11**: p. 816.

33. Haun, C.T., et al., *Muscle fiber hypertrophy in response to 6 weeks of high-volume resistance training in trained young men is largely attributed to sarcoplasmic hypertrophy.* PLoS One, 2019. **14**(6): p. e0215267.
34. Jorgenson, K.W., S.M. Phillips, and T.A. Hornberger, *Identifying the Structural Adaptations that Drive the Mechanical Load-Induced Growth of Skeletal Muscle: A Scoping Review.* Cells, 2020. **9**(7).
35. Libardi, C.A., et al., *Effects of low-load resistance training with blood flow restriction on muscle fiber myofibrillar and extracellular area.* Front Physiol, 2024. **15**: p. 1368646.
36. Monti, E., et al., *Are muscle fibres of body builders intrinsically weaker? A comparison with single fibres of aged-matched controls.* Acta Physiol (Oxf), 2021. **231**(2): p. e13557.
37. Lieber, R.L. and S.C. Bodine-Fowler, *Skeletal muscle mechanics: implications for rehabilitation.* Phys Ther, 1993. **73**(12): p. 844-56.
38. Rindom, E., et al., *Activation of mTORC1 signalling in rat skeletal muscle is independent of the EC-coupling sequence but dependent on tension per se in a dose-response relationship.* Acta Physiol (Oxf), 2019. **227**(3): p. e13336.
39. Navarro, A.P., M.A. Collins, and E.S. Folker, *The nucleus is a conserved mechanosensation and mechanoresponse organelle.* Cytoskeleton (Hoboken), 2016. **73**(2): p. 59-67.
40. Crossland, H., et al., *Focal adhesion kinase is required for IGF-I-mediated growth of skeletal muscle cells via a TSC2/mTOR/S6K1-associated pathway.* Am J Physiol Endocrinol Metab, 2013. **305**(2): p. E183-93.
41. Bodine, S.C., et al., *Akt/mTOR pathway is a crucial regulator of skeletal muscle hypertrophy and can prevent muscle atrophy in vivo.* Nat Cell Biol, 2001. **3**(11): p. 1014-9.
42. Hornberger, T.A., et al., *The role of phospholipase D and phosphatidic acid in the mechanical activation of mTOR signaling in skeletal muscle.* Proc Natl Acad Sci U S A, 2006. **103**(12): p. 4741-6.
43. You, J.S., et al., *The role of raptor in the mechanical load-induced regulation of mTOR signaling, protein synthesis, and skeletal muscle hypertrophy.* FASEB J, 2019. **33**(3): p. 4021-4034.
44. Hornberger, T.A., et al., *Mechanical stimuli regulate rapamycin-sensitive signalling by a phosphoinositide 3-kinase-, protein kinase B- and growth factor-independent mechanism.* Biochem J, 2004. **380**(Pt 3): p. 795-804.
45. von Walden, F., et al., *Mechanical loading induces the expression of a Pol I regulon at the onset of skeletal muscle hypertrophy.* Am J Physiol Cell Physiol, 2012. **302**(10): p. C1523-30.
46. West, D.W., et al., *Acute resistance exercise activates rapamycin-sensitive and -insensitive mechanisms that control translational activity and capacity in skeletal muscle.* J Physiol, 2016. **594**(2): p. 453-68.
47. Chaillou, T., et al., *Time course of gene expression during mouse skeletal muscle hypertrophy.* J Appl Physiol (1985), 2013. **115**(7): p. 1065-74.

48. Nakada, S., et al., *Correlation between Ribosome Biogenesis and the Magnitude of Hypertrophy in Overloaded Skeletal Muscle.* PLoS One, 2016. **11**(1): p. e0147284.
49. Millward, D.J., et al., *Relationship between protein synthesis and RNA content in skeletal muscle.* Nature, 1973. **241**(5386): p. 204-5.
50. Godwin, J.S., et al., *Skeletal muscle ribosome analysis: A comparison of common assay methods and utilization of a novel RiboAb antibody cocktail.* Physiol Rep, 2025. **13**(1): p. e70173.
51. Figueiredo, V.C. and J.J. McCarthy, *Regulation of Ribosome Biogenesis in Skeletal Muscle Hypertrophy.* Physiology (Bethesda), 2019. **34**(1): p. 30-42.
52. Hammarstrom, D., et al., *Benefits of higher resistance-training volume are related to ribosome biogenesis.* J Physiol, 2020. **598**(3): p. 543-565.
53. Mori, T., et al., *c-Myc overexpression increases ribosome biogenesis and protein synthesis independent of mTORC1 activation in mouse skeletal muscle.* Am J Physiol Endocrinol Metab, 2021. **321**(4): p. E551-E559.
54. Goodman, C.A., et al., *The role of skeletal muscle mTOR in the regulation of mechanical load-induced growth.* J Physiol, 2011. **589**(Pt 22): p. 5485-501.
55. Dumont, N.A., et al., *Satellite Cells and Skeletal Muscle Regeneration.* Compr Physiol, 2015. **5**(3): p. 1027-59.
56. McCarthy, J.J., et al., *Effective fiber hypertrophy in satellite cell-depleted skeletal muscle.* Development, 2011. **138**(17): p. 3657-66.
57. Englund, D.A., et al., *Satellite Cell Depletion Disrupts Transcriptional Coordination and Muscle Adaptation to Exercise.* Function (Oxf), 2021. **2**(1): p. zqaa033.
58. Fry, C.S., et al., *Regulation of the muscle fiber microenvironment by activated satellite cells during hypertrophy.* FASEB J, 2014. **28**(4): p. 1654-65.
59. Allen, D.L., R.R. Roy, and V.R. Edgerton, *Myonuclear domains in muscle adaptation and disease.* Muscle Nerve, 1999. **22**(10): p. 1350-60.
60. Pelland, J.C., et al., *The Resistance Training Dose Response: Meta-Regressions Exploring the Effects of Weekly Volume and Frequency on Muscle Hypertrophy and Strength Gains.* Sports Med, 2026. **56**(2): p. 481-505.
61. Robinson, Z.P., et al., *Exploring the Dose-Response Relationship Between Estimated Resistance Training Proximity to Failure, Strength Gain, and Muscle Hypertrophy: A Series of Meta-Regressions.* Sports Med, 2024. **54**(9): p. 2209-2231.
62. Refalo, M.C., et al., *Influence of Resistance Training Proximity-to-Failure on Skeletal Muscle Hypertrophy: A Systematic Review with Meta-analysis.* Sports Med, 2023. **53**(3): p. 649-665.
63. Hermann, T., et al., *Without Fail: Muscular Adaptations in Single-Set Resistance Training Performed to Failure or with Repetitions-in-Reserve.* Med Sci Sports Exerc, 2025. **57**(9): p. 2021-2031.
64. Carvalho, L., et al., *Muscle hypertrophy and strength gains after resistance training with different volume-matched loads: a systematic review and meta-analysis.* Appl Physiol Nutr Metab, 2022. **47**(4): p. 357-368.
65. Dankel, S.J., et al., *Muscle adaptations following 21 consecutive days of strength test familiarization compared with traditional training.* Muscle Nerve, 2017. **56**(2): p. 307-314.

66. Schoenfeld, B.J., et al., *Differential Effects of Heavy Versus Moderate Loads on Measures of Strength and Hypertrophy in Resistance-Trained Men*. J Sports Sci Med, 2016. **15**(4): p. 715-722.
67. Fink, J., et al., *Impact of high versus low fixed loads and non-linear training loads on muscle hypertrophy, strength and force development*. Springerplus, 2016. **5**(1): p. 698.
68. Schoenfeld, B.J., et al., *Effects of different volume-equated resistance training loading strategies on muscular adaptations in well-trained men*. J Strength Cond Res, 2014. **28**(10): p. 2909-18.
69. Weiss, L.W., H.D. Coney, and F.C. Clark, *Gross measures of exercise-induced muscular hypertrophy*. J Orthop Sports Phys Ther, 2000. **30**(3): p. 143-8.
70. Halperin, I., et al., *Accuracy in Predicting Repetitions to Task Failure in Resistance Exercise: A Scoping Review and Exploratory Meta-analysis*. Sports Med, 2022. **52**(2): p. 377-390.
71. Singer, A., et al., *Give it a rest: a systematic review with Bayesian meta-analysis on the effect of inter-set rest interval duration on muscle hypertrophy*. Front Sports Act Living, 2024. **6**: p. 1429789.
72. Pareja-Blanco, F., et al., *Effects of velocity loss during resistance training on athletic performance, strength gains and muscle adaptations*. Scand J Med Sci Sports, 2017. **27**(7): p. 724-735.
73. Plotkin, D.L., et al., *Hip thrust and back squat training elicit similar gluteus muscle hypertrophy and transfer similarly to the deadlift*. Front Physiol, 2023. **14**: p. 1279170.
74. Brandao, L., et al., *Varying the Order of Combinations of Single- and Multi-Joint Exercises Differentially Affects Resistance Training Adaptations*. J Strength Cond Res, 2020. **34**(5): p. 1254-1263.
75. Bloomquist, K., et al., *Effect of range of motion in heavy load squatting on muscle and tendon adaptations*. Eur J Appl Physiol, 2013. **113**(8): p. 2133-42.
76. Neilson, P.D., *The problem of redundancy in movement control: the adaptive model theory approach*. Psychol Res, 1993. **55**(2): p. 99-106.
77. Crowninshield, R.D. and R.A. Brand, *A physiologically based criterion of muscle force prediction in locomotion*. J Biomech, 1981. **14**(11): p. 793-801.
78. Latash, M.L., *The Hand: Shall We Ever Understand How it Works?* Motor Control, 2015. **19**(2): p. 108-26.
79. Gordon, A.M., A.F. Huxley, and F.J. Julian, *The variation in isometric tension with sarcomere length in vertebrate muscle fibres*. J Physiol, 1966. **184**(1): p. 170-92.
80. Maeo, S., et al., *Hamstrings Hypertrophy Is Specific to the Training Exercise: Nordic Hamstring versus Lengthened State Eccentric Training*. Med Sci Sports Exerc, 2024. **56**(10): p. 1893-1905.
81. Maeo, S., et al., *Triceps brachii hypertrophy is substantially greater after elbow extension training performed in the overhead versus neutral arm position*. Eur J Sport Sci, 2023. **23**(7): p. 1240-1250.

82. Larsen, S., et al., *Resistance Training Beyond Momentary Failure: The Effects of Past-Failure Partials Versus Initial Partials on Calf Muscle Hypertrophy Among a Resistance-Trained Cohort.* Eur J Sport Sci, 2025. **25**(9): p. e70030.
83. Pedrosa, G.F., et al., *Partial range of motion training elicits favorable improvements in muscular adaptations when carried out at long muscle lengths.* Eur J Sport Sci, 2022. **22**(8): p. 1250-1260.
84. Larsen, S., et al., *Knee flexion range of motion does not influence muscle hypertrophy of the quadriceps femoris during leg press training in resistance-trained individuals.* J Sports Sci, 2025. **43**(10): p. 986-994.
85. Sato, S., et al., *Elbow Joint Angles in Elbow Flexor Unilateral Resistance Exercise Training Determine Its Effects on Muscle Strength and Thickness of Trained and Non-trained Arms.* Front Physiol, 2021. **12**: p. 734509.
86. Varovic, D., et al., *Does Muscle Length Influence Regional Hypertrophy? A Systematic Review and Meta-Analysis.* Int J Sports Med, 2025. **46**(14): p. 1027-1036.
87. Newmire, D.E. and D.S. Willoughby, *The skeletal muscle microbiopsy method in exercise and sports science research: A narrative and methodological review.* Scand J Med Sci Sports, 2022. **32**(11): p. 1550-1568.
88. Sexton, C.L., et al., *Skeletal Muscle DNA Methylation and mRNA Responses to a Bout of Higher versus Lower Load Resistance Exercise in Previously Trained Men.* Cells, 2023. **12**(2).
89. Haun, C.T., et al., *Molecular, neuromuscular, and recovery responses to light versus heavy resistance exercise in young men.* Physiol Rep, 2017. **5**(18).
90. Michel, J.M., et al., *Effects of leg immobilization and recovery resistance training on skeletal muscle-molecular markers in previously resistance-trained versus untrained adults.* J Appl Physiol (1985), 2025. **138**(2): p. 450-467.
91. Wen, Y., et al., *MyoVision: software for automated high-content analysis of skeletal muscle immunohistochemistry.* J Appl Physiol (1985), 2018. **124**(1): p. 40-51.
92. Pillon, N.J., et al., *Transcriptomic profiling of skeletal muscle adaptations to exercise and inactivity.* Nat Commun, 2020. **11**(1): p. 470.
93. Pillon, N.J., et al., *Distinctive exercise-induced inflammatory response and exerkine induction in skeletal muscle of people with type 2 diabetes.* Sci Adv, 2022. **8**(36): p. eabo3192.
94. Gabriel, B.M., et al., *The Hippo signal transduction network for exercise physiologists.* J Appl Physiol (1985), 2016. **120**(10): p. 1105-17.
95. Lopez, P., et al., *Resistance Training Load Effects on Muscle Hypertrophy and Strength Gain: Systematic Review and Network Meta-analysis.* Med Sci Sports Exerc, 2021. **53**(6): p. 1206-1216.
96. Horwath, O., et al., *Variability in vastus lateralis fiber type distribution, fiber size, and myonuclear content along and between the legs.* J Appl Physiol (1985), 2021. **131**(1): p. 158-173.
97. Haun, C.T., et al., *A Critical Evaluation of the Biological Construct Skeletal Muscle Hypertrophy: Size Matters but So Does the Measurement.* Front Physiol, 2019. **10**: p. 247.

98. Ruple, B.A., et al., *Comparisons between skeletal muscle imaging techniques and histology in tracking midthigh hypertrophic adaptations following 10 wk of resistance training.* J Appl Physiol (1985), 2022. **133**(2): p. 416-425.
99. Haun, C.T., et al., *Pre-training Skeletal Muscle Fiber Size and Predominant Fiber Type Best Predict Hypertrophic Responses to 6 Weeks of Resistance Training in Previously Trained Young Men.* Front Physiol, 2019. **10**: p. 297.
100. Chen, X., et al., *Changes in sarcomere lengths of the human vastus lateralis muscle with knee flexion measured using in vivo microendoscopy.* J Biomech, 2016. **49**(13): p. 2989-2994.